

Adaptive Bayesian Joint Latent Space Modeling via Cumulative Shrinkage

Bin Lv, Yincai Tang, and Siliang Zhang*

Key Laboratory of Advanced Theory and Application in Statistics and Data Science-MOE, School of Statistics, East China Normal University

Abstract

Network models are increasingly vital in psychometrics for analyzing relational data, which are often accompanied by high-dimensional node attributes. Joint latent space models (JLSM) provide an elegant framework for integrating these data sources by assuming a shared underlying latent representation; however, a persistent methodological challenge is determining the dimension of the latent space, as existing methods typically require pre-specification or rely on computationally intensive post-hoc procedures. We develop a novel Bayesian joint latent space model that incorporates a cumulative ordered spike-and-slab (COSS) prior. This approach enables the latent dimension to be inferred automatically and simultaneously with all model parameters. We develop an efficient Markov Chain Monte Carlo (MCMC) algorithm for posterior computation. Theoretically, we establish that the posterior distribution concentrates on the true latent dimension and that parameter estimates achieve Hellinger consistency at a near-optimal rate that adapts to the unknown dimensionality. Through extensive simulations and two real-data applications, we demonstrate the method's superior performance in both dimension recovery and parameter estimation. Our work offers a principled, computationally efficient, and theoretically grounded solution for adaptive dimension selection in psychometric network models.

Keywords: Joint latent space model, latent dimension selection, spike-and-slab priors, psychometric network models

*Corresponding author: slzhang@fem.ecnu.edu.cn

1 Introduction

Network analysis has become an essential tool in psychometrics for understanding the structure of relationships that underpins psychological phenomena (Epskamp et al., 2017, 2018; Jeon et al., 2021; Borsboom et al., 2021). Its increasing adoption has spurred a rapid expansion of quantitative methods (Sweet, 2015; Liu et al., 2018; Sweet and Adhikari, 2020; Che et al., 2021; Liu et al., 2021), from Bayesian graphical models for ordinal data (Marsman et al., 2025) to specialized latent space approaches for item response data (Jin and Jeon, 2019; Jeon et al., 2021), alongside comprehensive surveys charting the progress (Sweet, 2016; Wang, 2021).

A frontier in this domain is the integration of network structures with the rich, often high-dimensional, attributes of the nodes themselves (McCallum et al., 2000; Leskovec and McAuley, 2012; Zhang et al., 2022). The interaction between these data sources is typically reciprocal. An individual's attributes influence their network position, while their network ties can shape their behaviors, a confounding that presents a modeling challenge (Fratiglioni et al., 2000; McPherson et al., 2001; Shalizi and Thomas, 2011; VanderWeele, 2011). This dynamic necessitates an integrated analytical framework, as modeling both data sources jointly is crucial for achieving a robust and comprehensive understanding of the underlying latent constructs (Zhang et al., 2016, 2022; Wang et al., 2023).

Latent space models (LSMs) offer powerful and interpretable tools for this purpose (Hoff et al., 2002). LSMs represent nodes as points in a low-dimensional geometric space, where proximity is proportional to the likelihood of a connection. This framework extends naturally to a *joint* LSM, where a *shared* latent space generates both the network ties and the node attributes (Gollini and Murphy, 2016; Salter-Townshend and McCormick, 2017; Wang et al., 2023). By unifying these data sources, JLSM can borrow statistical strength across them, yielding more robust and accurate estimates of the underlying structure than could be achieved by analyzing either data source in isolation.

Despite their power, LSMs face a fundamental and persistent challenge: the selection of the latent space dimension. This choice is not a mere technicality; it has implications for both statistical validity and substantive interpretation. An under-dimensioned model risks missing key structural features of the data (underfitting), while an over-dimensioned model is prone to capturing spurious noise (overfitting) and produces latent factors that are difficult to interpret. Standard practice involves fitting a series of models with different pre-specified dimensions and selecting the “best” one using post-hoc criteria like cross-validation or information criteria (e.g., AIC, BIC) (Hoff, 2007; Chen and Lei, 2018). These approaches are not only computationally prohibitive but also conceptually unsatisfying, as they sepa-

rate the crucial task of dimension selection from the main inferential procedure. Moreover, the dependency between data points in network data violates the assumptions of standard cross-validation, the effective number of parameters required for information criteria can be ambiguous, and the marginal log likelihood is difficult to calculate in the LSMs context (Spiegelhalter et al., 2002; Vaida and Blanchard, 2005; Li et al., 2020).

A fully Bayesian solution involves placing a prior over the latent dimension and inferring it alongside model parameters. However, this approach is not straightforward. Early attempts using ordered shrinkage priors (Bhattacharya and Dunson, 2011; Durante and Dunson, 2014) often induced excessive shrinkage and were sensitive to hyperparameters (Durante, 2017). More recent methods have advanced this goal by employing sophisticated shrinkage techniques. For instance, rotational strategies have shown promise in factor analysis (Ročková and George, 2016), and spike-and-slab priors have been successfully applied to related problems (Ishwaran and Rao, 2005; Guhaniyogi and Rodriguez, 2020; Guha and Rodriguez, 2021) and to network eigenmodels (Loyal and Chen, 2025). While the cumulative shrinkage process prior has also emerged as a powerful tool in Gaussian linear factor models (Legramanti et al., 2020; Schiavon et al., 2022), its empirical performance and theoretical properties are under-explored within the complex setting of joint network models.

In this work, we propose a Bayesian joint latent space model that automatically learns the effective number of latent dimensions from the data. Our approach incorporates a non-homogeneous cumulative shrinkage prior that automatically learns the effective number of latent dimensions from the data. This prior induces a stochastic ordering and progressively penalizes additional dimensions, allowing superfluous dimensions to fade during estimation. Our approach builds upon recent advancements in adaptive Bayesian shrinkage for latent variable models (Ročková and George, 2016; Legramanti et al., 2020; Schiavon et al., 2022; Li et al., 2025; Loyal and Chen, 2025).

The key contributions of our work are four-fold: (1) We introduce a novel, fully Bayesian joint LSM that seamlessly integrates parameter estimation and latent dimension selection into a single, coherent inferential framework. (2) We provide an efficient and adaptive Markov Chain Monte Carlo (MCMC) algorithm for posterior computation, making the approach practical for real-world applications. (3) We extend the Bayesian dimension selection framework to the joint LSMs, proving the posterior latent dimension concentrates round the true dimension and that the model parameters achieve a near-optimal Hellinger contraction rate that adapts to the unknown dimensionality. (4) We demonstrate through extensive simulations and two real-data applications that our method outperforms existing approaches in dimension recovery, parameter estimation accuracy, and computational efficiency.

The remainder of the article is structured as follows. In Section 2, we present the joint latent space model. In Section 3, we develop the novel cumulative ordered spike-and-slab prior that enables adaptive dimension selection. Section 4 details the MCMC algorithm for posterior computation. We then establish the theoretical underpinnings of our approach in Section 5, proving key asymptotic properties of the posterior. The method’s empirical performance is evaluated through extensive simulation studies in Section 6 and two real-data applications in Section 7. Finally, Section 8 provides a concluding discussion.

2 The Joint Latent Space Model

Let $\mathcal{G} = (\mathcal{V}, \mathcal{E})$ be an undirected network on a set of n nodes $\mathcal{V} = \{1, \dots, n\}$, where \mathcal{E} is the set of edges. The network structure is represented by a symmetric adjacency matrix $\mathbf{A} \in \{0, 1\}^{n \times n}$, where $A_{ii'} = 1$ if an edge exists between nodes i and i' , and $A_{ii'} = 0$ otherwise. In addition to the network, we observe a q -dimensional attribute vector $\mathbf{y}_i \in \mathbb{R}^q$ for each node i . These are collected in the matrix $\mathbf{Y} = [\mathbf{y}_1, \dots, \mathbf{y}_n]^\top \in \mathbb{R}^{n \times q}$.

We consider a joint latent space model that assumes the network \mathbf{A} and the node attributes \mathbf{Y} are generated from a common set of unobserved latent variables. Specifically, each node i is associated with a latent vector $\mathbf{z}_i \in \mathbb{R}^k$. The collection of these positions is denoted by the matrix $\mathbf{Z} = [\mathbf{z}_1, \dots, \mathbf{z}_n]^\top \in \mathbb{R}^{n \times k}$. The latent dimension k is unknown and a primary object of inference in our framework. The joint likelihood of the observed data (\mathbf{A}, \mathbf{Y}) is specified through two conditionally independent components given \mathbf{Z} .

Network Model For the adjacency matrix \mathbf{A} , we assume that the edges are conditionally independent given their latent positions. Specifically, for $1 \leq i < i' \leq n$, $A_{ii'} \sim \text{Bernoulli}(P_{ii'})$. We adopt the inner product formulation (Ma et al., 2020; Zhang et al., 2022) for its flexibility in modeling network structures:

$$\text{logit}(P_{ii'}) = \Theta_{ii'}^A = \alpha_i + \alpha_{i'} + \mathbf{z}_i^\top \mathbf{z}_{i'}, \quad (1)$$

where $\text{logit}(x) = \log\{x/(1-x)\}$. The parameters $\boldsymbol{\alpha} = (\alpha_1, \dots, \alpha_n)^\top$ capture node-specific degree heterogeneity; a larger α_i increases the propensity of node i to form connections. The inner product term $\mathbf{z}_i^\top \mathbf{z}_{i'}$ captures homophily and facilitates transitivity, as nodes with similar latent positions (yielding a larger inner product) are more likely to connect.

Node Attribute Model For the node attribute matrix \mathbf{Y} , we assume that the entries Y_{ij} are conditionally independent given \mathbf{Z} . Specifically, assume the distribution of Y_{ij} belongs

to the exponential family with natural parameter

$$\Theta_{ij}^Y = \gamma_j + \boldsymbol{\beta}_j^\top \mathbf{z}_i, \quad 1 \leq i \leq n, 1 \leq j \leq q. \quad (2)$$

Let $\boldsymbol{\gamma} = (\gamma_1, \dots, \gamma_q)^\top \in \mathbb{R}^q$ represents the intercept terms, and $\mathbf{B} = [\boldsymbol{\beta}_1, \dots, \boldsymbol{\beta}_q]^\top \in \mathbb{R}^{q \times k}$ is the matrix of regression coefficients, also interpreted as factor loadings. The density function Y_{ij} can be written as:

$$f(Y_{ij} | \mathbf{z}_i, \boldsymbol{\beta}_j, \gamma_j, \phi_j) = \exp \left\{ \frac{Y_{ij} \Theta_{ij}^Y - b(\Theta_{ij}^Y)}{\phi_j} + c(Y_{ij}, \phi_j) \right\},$$

where ϕ_j is a scale parameter, $b(\cdot)$ and $c(\cdot)$ are functions prespecified by a distribution. This framework encompasses many common models, including:

- **Linear Factor Model:** If Y_{ij} is continuous, assume

$$Y_{ij} | \mathbf{z}_i, \boldsymbol{\beta}_j, \gamma_j, \sigma_j^2 \sim \mathcal{N}(\gamma_j + \mathbf{z}_i^\top \boldsymbol{\beta}_j, \sigma_j^2),$$

which corresponds to the scale parameter $\phi_j = \sigma_j^2$.

- **Multidimensional Item Response Theory (MIRT) Model:** If Y_{ij} is binary, assume that

$$Y_{ij} | \mathbf{z}_i, \boldsymbol{\beta}_j, \gamma_j \sim \text{Bernoulli} \left(\frac{\exp(\gamma_j + \mathbf{z}_i^\top \boldsymbol{\beta}_j)}{1 + \exp(\gamma_j + \mathbf{z}_i^\top \boldsymbol{\beta}_j)} \right),$$

where the scale parameter $\phi_j = 1$.

Given the model specifications in (1) and (2), the joint likelihood of the observed data (\mathbf{A}, \mathbf{Y}) , conditional on the latent positions \mathbf{Z} and the model parameters $\{\boldsymbol{\alpha}, \boldsymbol{\gamma}, \mathbf{B}, \boldsymbol{\phi}\}$ ($\boldsymbol{\phi}$ denotes the scale parameters, if applicable), is formulated based on the assumption of conditional independence between the network and the node attributes, given the shared latent structure. The joint likelihood is the product of the likelihoods from the two components:

$$\begin{aligned} p(\mathbf{A}, \mathbf{Y} | \mathbf{Z}, \Xi) &= p(\mathbf{A} | \mathbf{Z}, \boldsymbol{\alpha}) p(\mathbf{Y} | \mathbf{Z}, \boldsymbol{\gamma}, \mathbf{B}, \boldsymbol{\phi}) \\ &= \left[\prod_{1 \leq i < i' \leq n} \frac{\exp(A_{ii'} \Theta_{ii'}^A)}{1 + \exp(\Theta_{ii'}^A)} \right] \times \left[\prod_{i=1}^n \prod_{j=1}^q \exp \left\{ \frac{Y_{ij} \Theta_{ij}^Y - b(\Theta_{ij}^Y)}{\phi_j} + c(Y_{ij}, \phi_j) \right\} \right]. \end{aligned} \quad (3)$$

This unified framework facilitates information sharing across data sources, thereby enhancing the robustness of the inference on the underlying latent structure. However, the model is subject to identifiability challenges inherent to latent variable models, where different

parameter configurations can produce the identical likelihood. Addressing these invariances is crucial for meaningful interpretation.

The first one is rotational invariance. Specifically, for any $k \times k$ orthogonal matrix \mathbf{Q} , the transformations $\mathbf{Z} \rightarrow \mathbf{Z}\mathbf{Q}$ and $\mathbf{B} \rightarrow \mathbf{B}\mathbf{Q}$ leave both the inner products $\mathbf{Z}\mathbf{Z}^\top$ and the linear predictors $\mathbf{Z}\mathbf{B}^\top$ in (3) unchanged. This rotational ambiguity, which includes column permutations (label switching) and sign-flips, implies that the latent coordinates and loadings are not uniquely identifiable from the likelihood alone. We address this through a cumulative ordered spike-and-slab prior detailed in Section 3. This prior induces a stochastic ordering on the variances of the latent dimensions, providing a soft identifiability constraint that breaks the symmetry and encourages an interpretable orientation aligned with decreasing explained variance. Second, to fix the origin of the latent space, we specify a zero-mean prior for each latent position, such that $\mathbb{E}(\mathbf{z}_i) = \mathbf{0}$.

We further remark that the assumption that models (1) and (2) share identical latent variables \mathbf{Z} can be relaxed, as stated in Zhang et al. (2022). Suppose the network \mathbf{A} is modeled by $\mathbf{Z}_A \in \mathbb{R}^{n \times k_A}$ via Eq. (1), and the attributes \mathbf{Y} are modeled by $\mathbf{Z}_Y \in \mathbb{R}^{n \times k_Y}$ via an exponential family model with natural parameter:

$$\Theta_{ij}^Y = \gamma_j + \mathbf{z}_{Y,i}^\top \boldsymbol{\beta}_j. \quad (4)$$

If the two latent spaces are related by an approximate linear transformation $\mathbf{Z}_Y \approx \mathbf{Z}_A \mathbf{W}$ for some transformation matrix $\mathbf{W} \in \mathbb{R}^{k_A \times k_Y}$, then Eq. (4) can be approximated as:

$$\Theta_{ij}^Y \approx \gamma_j + \mathbf{z}_{A,i}^\top (\mathbf{W}\boldsymbol{\beta}_j) = \gamma_j + \mathbf{z}_{A,i}^\top \boldsymbol{\beta}'_j,$$

where $\boldsymbol{\beta}'_j = \mathbf{W}\boldsymbol{\beta}_j$. Thus the joint model formulation remains a valid approximation even if the latent variables are not identical, provided one can be sufficiently described by another one through a linear mapping. In this context, \mathbf{Z} serves as the shared latent representation modeling both components.

We adopt a fully Bayesian approach for parameter estimation, treating the latent variables \mathbf{Z} and the parameters $\boldsymbol{\alpha}$, $\boldsymbol{\gamma}$, and \mathbf{B} as random variables. We specify the following conventional prior distributions to the model parameters: $\boldsymbol{\alpha} \sim \mathcal{N}(\mathbf{0}, \sigma_\alpha^2 \mathbf{I}_n)$, $\boldsymbol{\gamma} \sim \mathcal{N}(\mathbf{0}, \sigma_\gamma^2 \mathbf{I}_q)$, and $\beta_{jh} \sim \mathcal{N}(0, \sigma_B^2)$ for $j = 1, \dots, q$ and $h = 1, \dots, k$. For the linear factor model, we place an inverse-gamma prior on the noise variances: $\sigma_j^2 \sim \text{IG}(a_\sigma, b_\sigma)$. The prior for the latent variables \mathbf{Z} , which is central to our goal of inferring the dimension k , is detailed in the next section.

3 Adaptive Dimension Selection via Cumulative Shrinkage

A critical challenge in latent space modeling is the selection of the latent dimension k . A fixed, pre-specified k risks either underfitting by missing important structural features or overfitting by modeling spurious noise. To address this, we develop a Bayesian procedure that infers the effective number of latent dimensions directly from the data. Our approach begins by positing a model with a large, fixed number of potential latent dimensions. We then introduce a novel shrinkage prior on the columns of the latent variable matrix \mathbf{Z} that adaptively deactivates superfluous dimensions.

The key to our prior is the principle of ordered importance, where subsequent dimensions contribute progressively less explanatory power. We formalize this by constructing a non-homogeneous cumulative shrinkage process, which integrates a spike-and-slab framework with an ordered prior structure. This construction induces a stochastic ordering on the variance parameters of the latent dimensions, effectively shrinking the norms of unnecessary columns in \mathbf{Z} towards zero while robustly retaining the signal in the active dimensions. We first define this process as a general tool for ordered variable selection before demonstrating its specific application to latent space inference.

3.1 The Non-Homogeneous Spike-and-Slab Cumulative Shrinkage Process

We first introduce the general construction of the prior, which combines elements of spike-and-slab priors (Ishwaran and Rao, 2005) and the cumulative shrinkage process (Legramanti et al., 2020). Let $\{\theta_h\}_{h=1}^k$ be a sequence of parameters, which will later represent the variances of the latent columns. We assign them a spike-and-slab prior where the probability of being drawn from the spike increases with the index h :

$$\theta_h \mid \pi_h \sim (1 - \pi_h)P_{\text{slab}} + \pi_h P_{\text{spike}}, \quad (5)$$

where P_{slab} is a distribution for active (non-zero) parameters and P_{spike} is a distribution tightly concentrated at zero. The key step lies in the construction of the spike probabilities π_h . To enforce cumulative shrinkage, we require the sequence of spike probabilities to be stochastically increasing: $\pi_1 \leq \pi_2 \leq \dots \leq \pi_k$. We achieve this by using a **stick-breaking**

process:

$$\pi_h = \sum_{l=1}^h \omega_l, \quad \text{where } \omega_l = v_l \prod_{m=1}^{l-1} (1 - v_m). \quad (6)$$

The weights $\{\omega_l\}_{l=1}^k$ are constructed by sequentially breaking a stick of unit length. At each step l , a proportion v_l of the *remaining* stick is broken off, forming the weight ω_l . To induce the desired ordering, we specify the proportions $\{v_l\}$ as:

$$v_1 \sim \text{Beta}(\kappa, 1), \quad v_l \sim \text{Beta}(a, 1) \text{ for } l = 2, \dots, k-1, \quad \text{and } v_k = 1.$$

The weights ω_l define a probability mass function over the indices $\{1, \dots, k\}$, and π_h is the cumulative probability up to index h . The stick-breaking variables $v_l \in [0, 1]$ determine how the probability mass is allocated. The process is *non-homogeneous* because the distribution for the first break, governed by hyperparameter $\kappa > 0$, differs from that of subsequent breaks, governed by $a > 0$. By setting a large κ , we can encourage the first weight ω_1 to be small, thus making the first parameter θ_1 likely to be active (drawn from the slab). Conversely, larger values of a push subsequent weights towards zero, increasing the spike probability π_h more rapidly for larger h .

This construction leads to an ordering property, formalized below. Let the spike distribution be a point mass at zero, $P_{\text{spike}} = \delta_0$.

Proposition 1 (Stochastic Ordering) *Let $\{\theta_h\}_{h=1}^k$ follow the prior defined by (5)–(6) with $P_{\text{spike}} = \delta_0$. Then for any $\epsilon > 0$, $\Pr(|\theta_{h+1}| \leq \epsilon) > \Pr(|\theta_h| \leq \epsilon)$ for all $1 \leq h < k$.*

Proposition 1 confirms that the prior makes successive parameters stochastically smaller. That is, θ_{h+1} is more likely to be near zero than θ_h , formalizing the notion of ordered, adaptive shrinkage. Apart from the stochastic ordering, we further have that this prior exhibits exponentially decaying tails, provided the hyperparameters are chosen appropriately. This is crucial for establishing adaptive posterior contraction rates, and we refer readers to Lemma ?? in the Supplementary Material for details.

3.2 Prior Specification for the Latent Positions

We now apply this framework to specify the prior for the latent position matrix \mathbf{Z} . We assume that all latent positions z_{ih} in a given column h share a common variance parameter θ_h . The full hierarchical prior is:

$$\begin{aligned} z_{ih} \mid \theta_h &\sim \mathcal{N}(0, \theta_h), \quad \text{for } i = 1, \dots, n, \\ \theta_h \mid \pi_h &\sim (1 - \pi_h)\text{IG}(a_\theta, b_\theta) + \pi_h \delta_{\theta_0}, \end{aligned} \quad (7)$$

where the spike probabilities $\{\pi_h\}$ are generated by the non-homogeneous stick-breaking process in (6). The slab distribution is an Inverse-Gamma, a conventional choice for variances that is computationally convenient. The spike component, δ_{θ_0} , is a point mass at a small positive value $\theta_0 > 0$, representing a near-zero variance. In practice, setting θ_0 to a small, fixed positive value results in a continuous shrinkage prior, which can improve the mixing and stability of MCMC samplers by avoiding true zeros while still achieving effective dimension selection (Ishwaran and Rao, 2005; Legramanti et al., 2020). For subsequent theoretical analysis, we can consider the limiting case where the spike variance $\theta_0 \rightarrow 0$. We refer to the above hierarchical construction for the latent positions as the **Cumulative Ordered Spike-and-Slab (COSS) prior**.

A key feature of the COSS prior is the marginal distribution it induces on the latent positions z_{ih} after integrating out the random variances θ_h . This marginal is a two-component mixture:

$$z_{ih} \sim (1 - \pi_h)t_{2a_\theta}(0, b_\theta/a_\theta) + \pi_h\mathcal{N}(0, \theta_0),$$

where $t_{2a_\theta}(0, b_\theta/a_\theta)$ denotes a Student's t -distribution with $2a_\theta$ degrees of freedom, mean zero, and scale parameter $\sqrt{b_\theta/a_\theta}$. The slab component is heavy-tailed, which provides robustness by preventing excessive shrinkage of genuinely large latent positions. The spike component is a narrow Gaussian, which strongly pulls irrelevant positions towards zero.

This prior on \mathbf{Z} directly inherits the ordering property from Proposition 1, which is crucial for resolving the inherent column permutation invariance of the latent space likelihood.

Corollary 1 (Stochastic Ordering of Latent Positions) *Let z_{ih} be drawn from the COSS prior defined in (7). For any $\epsilon > 0$, the inequality $\Pr(|z_{i,h+1}| \leq \epsilon) > \Pr(|z_{ih}| \leq \epsilon)$ holds for all $1 \leq h < k$, provided that the spike component is more concentrated around zero than the slab component.¹*

The columns of \mathbf{Z} are stochastically ordered, with columns of higher index being progressively shrunk towards zero. This soft constraint encourages the model to allocate variance to the first few latent dimensions before activating later ones, providing a practical solution for adaptive dimension selection.

¹A sufficient condition for this is that the variance of the spike is smaller than the variance of the slab $\theta_0 < b_\theta/a_\theta$, which is ensured by hyperparameter choice.

4 Posterior Computation

We develop an efficient Markov Chain Monte Carlo (MCMC) algorithm for posterior inference of the joint latent space model equipped with the cumulative shrinkage prior. The algorithm is based on a Gibbs sampler that leverages data augmentation and an adaptive truncation scheme to efficiently explore the posterior distribution of both the parameters and the latent dimension. We first describe the sampler for a fixed truncation level k and then introduce an adaptive scheme that allows k to be adjusted dynamically during sampling, enhancing computational efficiency.

4.1 Posterior Computation via Gibbs Sampling

The primary challenges in posterior sampling arise from the non-conjugacy induced by the logistic network model (1) and the complex structure of the COSS prior (7). We address these challenges using two key strategies.

To address the non-conjugacy induced by the logistic likelihood of the network component, we employ the Pólya-Gamma data augmentation scheme of Polson et al. (2013). This approach leverages the following integral representation of the logistic function:

$$\frac{(e^\phi)^a}{(1 + e^\phi)^b} = 2^{-b} e^{\kappa\phi} \int_0^\infty e^{-\frac{\tau\phi^2}{2}} p(\tau; b, 0) d\tau, \quad (8)$$

where $\kappa = a - b/2$ and $p(\tau; b, 0)$ denotes the density for the Pólya-Gamma random variable τ . The introduction of the Pólya-Gamma latent variables induces conditional conjugacy, enabling updates of the network parameters $\boldsymbol{\alpha}$ and latent positions \mathbf{Z} from normal distributions within a Gibbs sampling framework. The sampling procedure and its detailed derivation are provided in Algorithm 1 and Section A of the Supplementary Material, respectively.

Next, in order to efficiently sample the parameters of the COSS prior, we introduce discrete random variable $\rho_h \in \{1, \dots, k\}$ such that $\Pr(\rho_h = l \mid \boldsymbol{\omega}) = \omega_l$. Thus the conditional distribution for the variance parameter θ_h in (7) can be rewritten as:

$$\theta_h \mid \rho_h \sim \{1 - \mathbb{1}(\rho_h \leq h)\} \text{IG}(a_\theta, b_\theta) + \mathbb{1}(\rho_h \leq h) \delta_{\theta_0}, \quad (9)$$

where $\mathbb{1}(\cdot)$ denotes the indicator function. If $\rho_h \leq h$, the dimension is assigned to the spike; otherwise, it is assigned to the slab. Moreover, let $K^* = \sum_{h=1}^k \mathbb{1}(\rho_h > h)$ that counts the number of active elements in $\boldsymbol{\theta}$, which is referred to as the active dimension afterwards.

The indicators ρ_h are updated by sampling from a categorical distribution whose probabilities are derived by marginalizing θ_h from the joint density of the latent positions $\mathbf{Z}_{.h}$ (the

h th column of \mathbf{Z}). The conditional posterior probabilities are:

$$\Pr(\rho_h = l \mid \text{rest}) \propto \begin{cases} \omega_l \mathcal{N}(\mathbf{Z}_{\cdot h}; \mathbf{0}, \theta_0 \mathbf{I}_n), & \text{if } l \leq h, \\ \omega_l t_{2a_\theta}(\mathbf{Z}_{\cdot h}; \mathbf{0}, (b_\theta/a_\theta) \mathbf{I}_n), & \text{if } l > h. \end{cases} \quad (10)$$

This mixture representation, involving a narrow Gaussian (spike) and a heavy-tailed Student-t distribution (slab, resulting from integrating the Inverse-Gamma prior), allows for efficient updates while enabling robust shrinkage.

The Gibbs sampler proceeds by iteratively updating the network parameters $(\boldsymbol{\alpha}, \mathbf{Z})$, the node attribute parameters (e.g., $\boldsymbol{\gamma}, \mathbf{B}, \boldsymbol{\sigma}^2$ for the linear factor model), and the parameters of the shrinkage prior $(\boldsymbol{\theta}, \boldsymbol{\rho}, \boldsymbol{v}, \boldsymbol{\omega})$. Algorithm 1 summarizes the steps for the joint model with Gaussian node attributes. Detailed derivations and the algorithm for Bernoulli node variables (MIRT model), which requires an additional layer of Pólya-Gamma augmentation, are provided in the Supplementary Material.

4.2 Adaptive Truncation for Computational Efficiency

The theoretical guarantees in Section 5 require the truncation level k to be large, potentially growing with n . However, in practice, the true dimension k_0 is usually much smaller than n . Running the sampler with a large, fixed k leads to significant computational inefficiency, as most of the computational effort is dedicated to updating parameters for inactive (spike) dimensions.

To maintain computational efficiency without sacrificing theoretical rigor, we adopt an adaptive Gibbs sampling strategy (Bhattacharya and Dunson, 2011; Legramanti et al., 2020) that dynamically adjusts the truncation level k during the MCMC iterations. At each iteration t (after the burn-in period \bar{t}), the sampler proposes to either expand or contract the latent space with a small and diminishing probability $p(t) = \exp(\eta_0 + \eta_1 t)$ ($\eta_0 \leq 0, \eta_1 < 0$). The adaptation procedure works as follows:

1. **Calculate active dimension:** $K^* = \sum_{h=1}^k \mathbb{1}(\rho_h > h)$.
2. **Contraction:** If more than one columns are currently inactive (i.e., $K^* < k-1$), reduce it to $k_{\text{new}} = K^* + 1$ and discard the parameters associated with columns $h > k_{\text{new}}$.
3. **Expansion:** If all current columns are active (i.e., $K^* = k$), add it to $k_{\text{new}} = k + 1$, sampling the parameters for the new dimension from their respective priors.

This adaptation, formalized in Algorithm 2, ensures that the sampler explores dimensions as needed without the high computational cost of a large, fixed k . The diminishing probability of

Algorithm 1 Sampling procedure for the joint latent space model (Gaussian)

Input: Observed data \mathbf{A} and \mathbf{Y}

Part 1: Update network parameters (α, \mathbf{Z}) and augmentation data
for $i = 1$ to n **do**

 Update augmentation data: For $i' \neq i$, sample $d_{ii'}^A \sim \text{PG}(1, \Theta_{ii'}^A)$.

 Update α_i : Sample from its Gaussian full conditional. (Details in Supp. Mat.).

 Update \mathbf{z}_i : Sample from its Gaussian full conditional. (Details in Supp. Mat.).

end for

Part 2: Update node parameters ($\gamma, \mathbf{B}, \sigma^2$)

 Update γ : Sample from its Gaussian full conditional. (Details in Supp. Mat.).

for $j = 1$ to q **do**

 Update β_j : Sample from $\mathcal{N}(M_{\beta_j}, V_{\beta_j})$, where $V_{\beta_j} = (\sigma_B^{-2}\mathbf{I}_k + \sigma_j^{-2}\mathbf{Z}^\top\mathbf{Z})^{-1}$ and $M_{\beta_j} = V_{\beta_j}\mathbf{Z}^\top\sigma_j^{-2}(\mathbf{Y}_{\cdot j} - \gamma_j\mathbf{1}_n)$.

 Update σ_j^2 : Sample from $\text{IG}(a_\sigma + n/2, b_\sigma + 0.5\|\mathbf{Y}_{\cdot j} - \gamma_j\mathbf{1}_n - \mathbf{Z}\beta_j\|_2^2)$.

end for

Part 3: Update shrinkage hyperparameters (ρ, θ, v, ω)

for $h = 1$ to k **do**

 Sample ρ_h from the categorical distribution defined by Eq. (10).

if $\rho_h \leq h$ (Spike) **then**

 Set $\theta_h = \theta_0$.

else

 Sample $\theta_h \sim \text{IG}(a_\theta + n/2, b_\theta + 0.5\|\mathbf{Z}_{\cdot h}\|_2^2)$.

end if

end for

Update stick-breaking variables v_1, \dots, v_{k-1} from their respective Beta conditionals.

Compute ω using Eq. (6).

adaptation satisfies the conditions of Roberts and Rosenthal (2007), ensuring the ergodicity of the Markov chain.

This fully Bayesian framework offers several advantages. First, the incorporation of the COSS prior allows for automatic and adaptive inference of the latent dimension k , integrating dimension selection within the estimation procedure rather than relying on computationally intensive post-hoc criteria as in frequentist approaches (Zhang et al., 2022; Wang et al., 2023). Second, the model structure and prior specification facilitate the construction of an efficient Gibbs sampler using data augmentation techniques, avoiding reliance on numerical approximations such as variational inference or Laplace approximations. Finally, we establish strong theoretical guarantees, demonstrating that the posterior distribution concentrates consistently on low-dimensional structures near the true model, as detailed in the next section.

Algorithm 2 Adaptive Gibbs Sampler with Dynamic Truncation

```
1: Input: Last truncation index  $k^{(t-1)}$ , total iteration  $T$ , burn-in  $\bar{t}$ , adaptation schedule
   parameters  $\eta_0, \eta_1$ .
2: for  $t = 1$  to  $T$  do
3:   Execute one cycle of Algorithm 1 with current truncation  $k^{(t-1)}$ .
4:   if  $t > \bar{t}$  and  $\text{Uniform}(0,1) < \exp(\eta_0 + \eta_1 t)$  then
5:     Determine the number of active columns,  $K^{*(t)} = \sum_{h=1}^{k^{(t-1)}} \mathbb{1}(\rho_h^{(t)} > h)$ .
6:     if  $K^{*(t)} < k^{(t-1)}$  then
7:       Set the new truncation level  $k^{(t)} = K^{*(t)} + 1$ .
8:       Drop all inactive columns from  $\mathbf{Z}$  and  $\mathbf{B}$  and their associated prior parameters.
9:     else
10:    Set  $k^{(t)} = k^{(t-1)} + 1$ .
11:    Add a new column to  $\mathbf{Z}$  and  $\mathbf{B}$ , initialized from the spike distribution.
12:  end if
13: else
14:   Set  $k^{(t)} = k^{(t-1)}$  (no adaptation).
15: end if
16: end for
17: Output: One posterior sample and the current truncation level  $k^{(t)}$ .
```

5 Theoretical Guarantees

This section provides theoretical justification for the proposed Bayesian joint latent space model, focusing on two key aspects: the ability of the posterior distribution to recover the true latent dimension and the accuracy of parameter estimation. We investigate the asymptotic consistency of the posterior as the number of nodes n increases.

We assume the data (\mathbf{A}, \mathbf{Y}) are generated from the models defined in (1) and (2) under a true set of parameters $\{\boldsymbol{\alpha}_0, \boldsymbol{\gamma}_0, \mathbf{B}_0, \boldsymbol{\phi}_0\}$ and a true latent dimension k_0 . Denote the expectation under this true process by \mathbb{E}_0 . To establish our theoretical results, we rely on several standard regularity conditions concerning the data generating process and prior specification. These conditions align with the literature on latent space models and high-dimensional Bayesian statistics (e.g., Ma et al., 2020; Zhang et al., 2022). Specifically, the prior truncation level k grows polynomially with n (i.e., $k \asymp n^\lambda$ for $\lambda \in (0, 1]$), while the true dimension k_0 grows much slower than k . This condition is easily met if k_0 is assumed fixed. Furthermore, we allow q to be high-dimensional, growing at most linearly with n . Finally, we impose standard boundedness conditions on the true parameters and mild conditions on the link function $f(Y_{ij} | \cdot)$. A formal statement of these assumptions and the required prior specifications is provided in the Supplementary Material.

5.1 Consistency of Latent Dimension Selection

Our first main result concerns the posterior distribution of the active latent dimension K^* . We demonstrate that the COSS prior effectively controls the complexity of the latent space, ensuring the estimated dimension does not significantly overshoot the true dimension k_0 .

Theorem 1 (Posterior Concentration for the Latent Dimension) *Consider the joint latent space model defined in Eqs. (1) and (2) with the cumulative shrinkage prior (7) placed on \mathbf{Z} , and standard Gaussian priors for $\boldsymbol{\alpha}, \boldsymbol{\gamma}, \mathbf{B}$. Under the regularity conditions detailed in the Supplementary Material, there exists a constant $C_1 > 1$ such that*

$$\lim_{n \rightarrow \infty} \mathbb{E}_0^{(n)} \{ \Pr(K^* > C_1 k_0 \mid \mathbf{A}, \mathbf{Y}) \} = 0.$$

Theorem 1 states that the posterior probability of overestimating the true latent dimension k_0 by more than a constant factor vanishes as the sample size grows. While this does not guarantee that the posterior mode will be exactly equal to k_0 in all finite samples, it ensures that the posterior mass concentrates on low-dimensional spaces that are asymptotically bounded relative to the true complexity. It demonstrates that the COSS prior is able to automatically penalize and discard superfluous dimensions, ensuring the posterior concentrates on parsimonious models. Therefore, practitioners can confidently set k sufficiently large and rely on the prior to automatically control model complexity.

5.2 Posterior Contraction Rate

Next, we establish the consistency of the posterior distribution for the model parameters and the rate at which it contracts around the truth. We measure the accuracy of the overall model fit using the Hellinger distance, which quantifies the discrepancy between the estimated probability distribution and the true one.

Theorem 2 (Adaptive Posterior Contraction Rate) *Let $\boldsymbol{\Theta} = \{\boldsymbol{\Theta}^A, \boldsymbol{\Theta}^Y\}$ represents the model natural parameters defined in Section 2. Under the same conditions as Theorem 1, the posterior distribution contracts around the true parameters $\boldsymbol{\Theta}_0 = \{\boldsymbol{\Theta}_0^A, \boldsymbol{\Theta}_0^Y\}$ at the rate $\epsilon_n = \sqrt{k_0 \log k/n}$, that is:*

$$\lim_{n \rightarrow \infty} \mathbb{E}_0^{(n)} [\Pr \{ H_n(\boldsymbol{\Theta}, \boldsymbol{\Theta}_0) > C_2 \epsilon_n \mid \mathbf{A}, \mathbf{Y} \}] = 0,$$

where k_0, k are the true and pre-specified latent dimensions. $H_n(\cdot, \cdot)$ is the root-averaged-squared Hellinger metric defined in the Supplementary Material and $C_2 > 0$ is a constant.

Theorem 2 establishes that the posterior distribution contracts around the true parameters at the rate ϵ_n . This rate is nearly identical to the minimax optimal rate k_0/n established for latent space models where the dimension k_0 is assumed known (Ma et al., 2020; Xie and Xu, 2020; Zhang et al., 2022). The extra logarithmic factor ($\log k$) is the statistical price paid for not knowing k_0 in advance (Loyal and Chen, 2025). Furthermore, the contraction rate adapts to the unknown true dimension k_0 . This means the model achieves high estimation accuracy without requiring prior knowledge of the latent space complexity. Furthermore, this result confirms that choosing a large truncation level k (which only appears in the logarithmic factor) does not substantially hinder the estimation accuracy, reinforcing the robustness of the proposed method.

This general guarantee of distributional convergence can be translated into more interpretable metrics for specific models. For instance, for binary node attributes (the MIRT model), we can show that the estimated probabilities converge to the true probabilities in terms of the Frobenius norm, see Corollary ?? in the Supplementary Material.

6 Simulations

We conducted simulation studies to evaluate the performance of the proposed joint latent space model equipped with the COSS prior. The simulations aimed to (1) assess the improvement in parameter recovery achieved by the JLSM compared to modeling the network and node attributes separately, and (2) benchmark the accuracy of the proposed dimension selection approach against standard model selection techniques. We investigated these aspects under varying sample sizes and network densities.

6.1 Study 1

6.1.1 Design and evaluation criteria

In this study, we evaluated the proposed method for estimating accuracy of parameter estimation, latent dimension recovery, and model selection under different sample sizes and model specifications. Data were generated from the joint latent space model under conditions reflecting different sample sizes and numbers of node attributes, with (n, q) pairs set to $(50, 10)$, $(100, 20)$, $(150, 30)$, and $(300, 60)$. The true latent dimension was fixed at $k_0 = 3$. For each of the 100 replications per condition, model parameters were drawn as follows: node heterogeneity parameters were drawn from $\alpha_i \sim U[-0.5, 0.5]$, resulting in relatively sparse networks (average density around 0.07), which presents a challenging scenario for latent space

recovery; intercept parameters were drawn from $\gamma_j \sim \mathcal{N}(0, 1)$; latent positions were generated independently from $z_{ih} \sim \mathcal{N}(0, 1)$; and a sparse loading matrix $\mathbf{B}_0 \in \mathbb{R}^{q \times k_0}$ of simple structure, where each row contained exactly one non-zero element drawn from $U[0.25, 1.25]$. The network adjacency matrix \mathbf{A} was generated from Eq. (1), and the node attribute matrix \mathbf{Y} was generated for two scenarios: continuous (Gaussian) and binary (Bernoulli) variables.

We compared the performance of our proposed Joint LSM to two specialized variants: a Network-Only LSM using only \mathbf{A} , and a Node-Only model (factor analysis or MIRT) using only \mathbf{Y} . The COSS prior was implemented in all three models. For MCMC settings, all models with the COSS prior were run for 15,000 iterations after a 10,000-iteration burn-in, with a thinning interval of five.

For implementation, the truncation level was initialized at $k = 8$. Hyperparameters were set as $a_\theta = b_\theta = 3$ and $a = 8$. The spike variance θ_0 was 0.1 for the Network LSM and JLSM, and 0.05 for the Node LVM. Weakly informative priors were used for other parameters ($\sigma_\alpha = \sigma_\gamma = 100$, $\sigma_B = 1$). The MCMC algorithms were run for 25,000 total iterations, with 10,000 discarded as burn-in, and the remainder thinned every 5 iterations, yielding 3,000 posterior samples. Adaptive Gibbs sampling was initiated after $\bar{t} = 500$ iterations, with adaptation parameters $(\eta_0, \eta_1) = (-1, -5 \times 10^{-4})$.

We evaluated performance using several normalized metrics calculated using posterior means. To assess the recovery of the latent structure, we used the normalized Frobenius error of the inner product matrix, $\Delta_Z = \|\hat{\mathbf{Z}}\hat{\mathbf{Z}}^\top - \mathbf{Z}_0\mathbf{Z}_0^\top\|_F/n$. Similarly, loading matrix estimation was evaluated by $\Delta_B = \|\hat{\mathbf{B}}\hat{\mathbf{B}}^\top - \mathbf{B}_0\mathbf{B}_0^\top\|_F/q$. The use of inner products accounts for the rotational invariance of the latent space. Parameter estimation accuracy for node heterogeneity and intercepts were measured by their normalized L_2 errors, $\Delta_\alpha = \|\hat{\boldsymbol{\alpha}} - \boldsymbol{\alpha}_0\|_2/\sqrt{n}$ and $\Delta_\gamma = \|\hat{\boldsymbol{\gamma}} - \boldsymbol{\gamma}_0\|_2/\sqrt{q}$, respectively. For dimension recovery, the latent dimension was estimated using the posterior mode,

$$\hat{K} = \operatorname{argmax}_l \hat{\Pr}(K^* = l \mid \mathbf{A}, \mathbf{Y}).$$

We report the accuracy (Acc; proportion of replications where $\hat{K} = k_0$) and the mean absolute bias (MAB), calculated only over replications where $\hat{K} \neq k_0$.

6.1.2 Results

The results of parameter recovery are summarized in Table 1, demonstrating a clear advantage for the joint modeling approach as well as the validity of the proposed dimension selection approach. The JLSM consistently outperforms both the Network LSM and the

Node LVM across all configurations and metrics. This demonstrates the statistical efficiency gained by integrating both data sources, allowing the model to borrow strength and yield more accurate estimates of the shared latent structure and associated parameters. As expected, estimation accuracy improves as the sample size increases, and performance is generally better with Gaussian attributes than Bernoulli attributes, reflecting the higher information content of continuous data.

Figure 1 illustrates the frequency of dimension selection across the three models. As the sample size increases, the accuracy of all models improves significantly, showing the consistency of the latent dimension selection. Moreover, the Joint LSM identified the true latent dimension with higher accuracy than the specialized models, especially in smaller samples.

We further compared the dimension selection performance of the COSS prior against standard post-hoc criteria. These benchmarks involved fitting a standard JLSM with independent $\mathcal{N}(0, 1)$ priors on z_{ih} across a range of fixed dimensions and selecting the optimal dimension using information criteria (AIC, BIC, DIC, WAIC) and K-fold cross-validation (K-fold CV) with $K = 5$ folds, where we selected the dimension maximizing the average held-out log-likelihood. We also considered the “K-fold CV 1SE” criterion to favor parsimony by selecting the smallest model within one standard deviation of the best model. See the Supplementary Material for more details on the criteria calculation.

Figure 2 compares the dimension selection performance of the COSS prior (labeled “Proposed”) against competing methods. The COSS prior was highly accurate and robust across all conditions. In contrast, traditional criteria exhibit notable biases: DIC and K-fold CV consistently overestimate the latent dimension. WAIC also tends to overestimate in small samples. Conversely, BIC often underestimates the dimension when the sample size is small ($n = 50$) but improves as n increases. AIC performs reasonably well, though it is slightly outperformed by the proposed method in small sample scenarios. Overall, the cumulative shrinkage prior provides robust and accurate dimension selection. Crucially, it achieves this within a single MCMC run, making it computationally more efficient than methods requiring fitting multiple models, and it naturally incorporates uncertainty about the latent dimension into the posterior inference.

6.2 Study 2

In the second study, we investigated the impact of network density on estimation accuracy, focusing on the ability of the joint model to leverage node attributes when network information is scarce. We fixed the sample size to $(n, q) = (100, 20)$ and $k_0 = 3$. We varied the

Table 1: Parameter recovery simulation results for true $k_0 = 3$. Values are means over 100 replications, with standard errors in parentheses. The values in the parentheses of the ‘Acc’ column are the mean absolute bias (MAB) calculated only when $\hat{K} \neq k_0$.

Y	(n, q)	Model	Δ_α	Δ_γ	Δ_B	Δ_Z	Acc (MAB)
Gaussian	(50,10)	Network	0.470(0.089)	–	–	1.067(0.116)	0.680(1.000)
		Node LVM	–	0.188(0.047)	0.335(0.060)	1.676(0.190)	0.000(2.640)
		JLSM	0.457(0.053)	0.193(0.056)	0.213(0.050)	0.954(0.113)	0.760(1.125)
	(100,20)	Network	0.318(0.050)	–	–	0.758(0.072)	1.000(0.000)
		Node LVM	–	0.123(0.027)	0.266(0.043)	1.443(0.184)	0.000(2.000)
		JLSM	0.310(0.046)	0.128(0.029)	0.135(0.021)	0.655(0.067)	1.000(0.000)
	(150,30)	Network	0.261(0.044)	–	–	0.619(0.051)	1.000(0.000)
		Node LVM	–	0.101(0.019)	0.312(0.039)	1.223(0.227)	0.210(1.468)
		JLSM	0.256(0.043)	0.107(0.024)	0.102(0.011)	0.535(0.045)	1.000(0.000)
	(300,60)	Network	0.187(0.031)	–	–	0.445(0.032)	1.000(0.000)
		Node LVM	–	0.075(0.013)	0.086(0.022)	0.715(0.100)	0.920(1.000)
		JLSM	0.183(0.030)	0.078(0.017)	0.068(0.005)	0.379(0.032)	1.000(0.000)
Bernoulli	(50,10)	Network	0.453(0.081)	–	–	1.042(0.107)	0.770(1.000)
		Node LVM	–	0.456(0.377)	0.514(0.220)	1.718(0.158)	0.000(2.080)
		JLSM	0.451(0.081)	0.428(0.349)	0.319(0.064)	1.025(0.112)	0.780(1.000)
	(100,20)	Network	0.322(0.053)	–	–	0.759(0.062)	0.980(1.000)
		Node LVM	–	0.286(0.056)	0.375(0.076)	1.689(0.136)	0.001(2.030)
		JLSM	0.322(0.052)	0.280(0.057)	0.249(0.033)	0.741(0.064)	0.980(1.000)
	(150,30)	Network	0.265(0.041)	–	–	0.628(0.046)	1.000(0.000)
		Node LVM	–	0.225(0.041)	0.312(0.039)	1.600(0.114)	0.090(1.747)
		JLSM	0.264(0.040)	0.216(0.035)	0.215(0.023)	0.612(0.046)	1.000(0.000)
	(300,60)	Network	0.180(0.025)	–	–	0.440(0.027)	1.000(0.000)
		Node LVM	–	0.168(0.020)	0.198(0.016)	1.301(0.071)	0.920(1.000)
		JLSM	0.178(0.025)	0.151(0.018)	0.156(0.015)	0.426(0.027)	1.000(0.000)

network density by adjusting the distribution of the node heterogeneity parameters α . By shifting the distribution of α_i from $U[-3, -1]$ (sparse) towards $U[-0.375, -0.125]$ (dense), we generated networks with densities ranging from 0.07 to 0.42. All other data-generating parameters and MCMC settings were identical to those in Study 1. We compared the performance of the JLSM and the Network LSM.

Figure 3 illustrates the latent structure recovery error (Δ_Z) and the dimension recovery accuracy (Acc) as a function of network density. The performance of the Network-Only LSM was highly dependent on network density. As the network became sparser (moving from right to left on the x-axis), the performance of the Network LSM deteriorates significantly across both metrics. In particular, in highly sparse regimes (e.g., density below 0.10), the Network LSM exhibits substantial estimation error, and its dimension recovery accuracy drops sharply to below 40%. This is expected, as sparse networks offer limited information for identifying

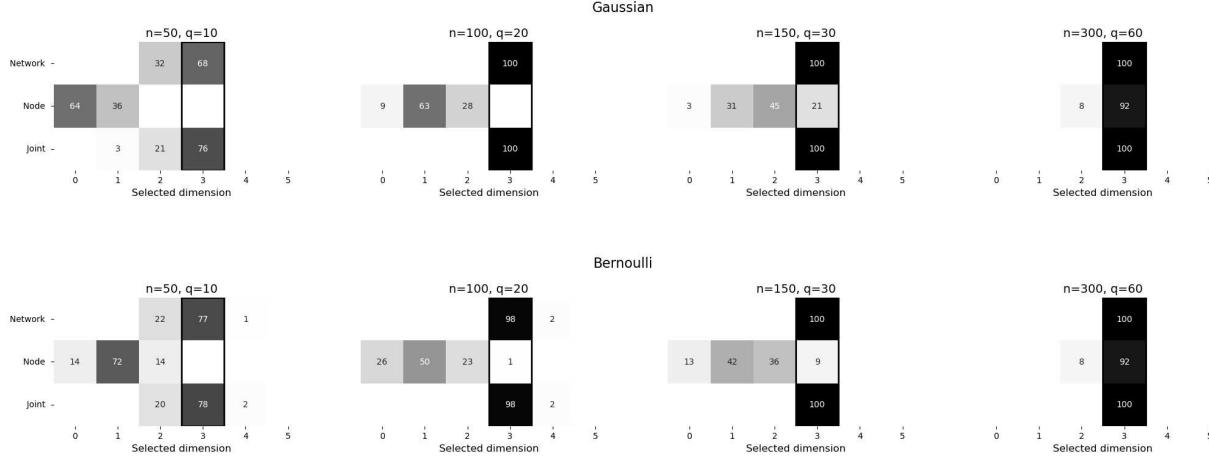


Figure 1: Frequency of dimension selection across 100 simulations for the three models using the COSS prior. The column outlined in black indicates the true value $k_0 = 3$. Darker cells indicate higher percentages.

the underlying latent space structure and its dimensionality.

In contrast, the Joint LSM performed consistently well across all levels of network density. Notably, the JLSM maintains significantly higher accuracy in dimension selection (over 65% for Gaussian and 70% for Bernoulli) even at the lowest densities tested. This stability arises because the model effectively borrows information from the node attributes when the network signal is weak. The attributes provide the necessary data to identify the true latent dimension and estimate the model parameters accurately. This finding highlights a key practical advantage of our approach: it ensures reliable adaptive dimension selection even when one data source is uninformative, a common challenge in applied research.

7 Real Data Analysis

We demonstrate the utility of the proposed joint latent space model (JLSM) with COSS priors through two empirical applications. The first analyzes the structure of a friendship network among French financial elites, illustrating the model’s ability to select the latent dimension and uncover meaningful social structures. The second evaluates the model’s performance in imputing missing node attributes in Facebook ego-networks, highlighting the predictive benefits of integrating network and attribute data.

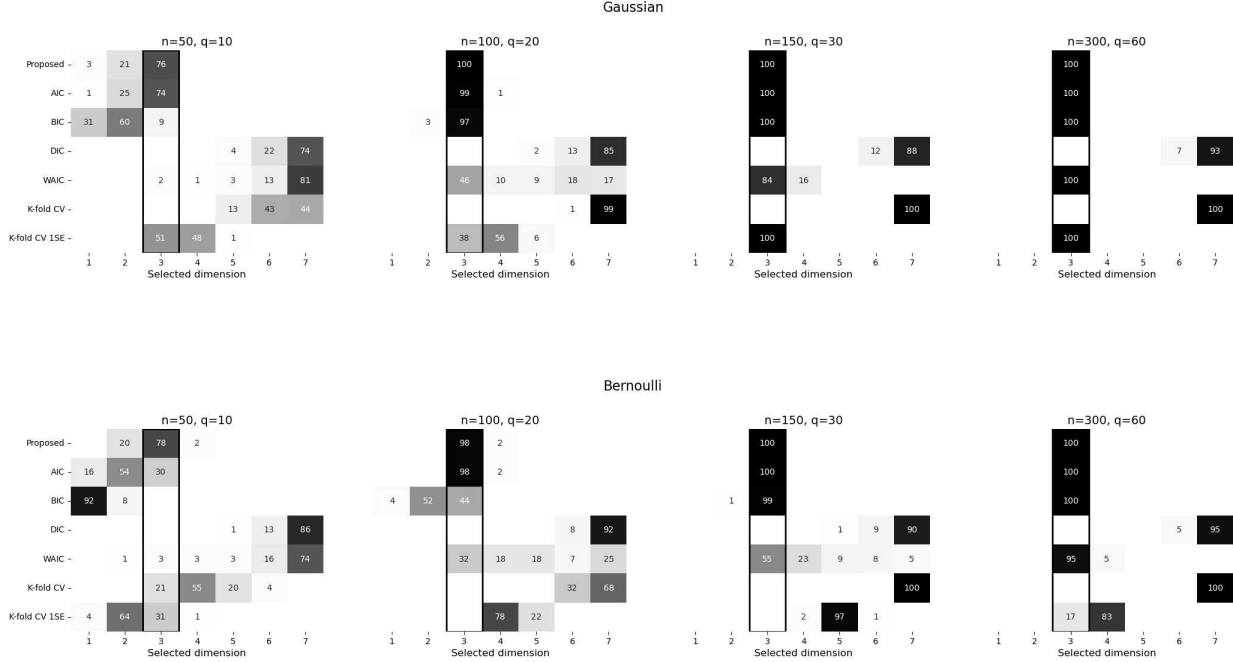


Figure 2: Comparison of dimension selection methods applied to the JLSM across 100 simulations. The column outlined in black indicates the true value $k_0 = 3$. Darker cells indicate higher percentages.

7.1 French Financial Elites Network

First we analyze the French financial elites dataset, originally collected by Kadushin (1995) to study social connections among top financial leaders during the final years of France’s Socialist government. This dataset has also been analyzed by Wang et al. (2023). The dataset comprises a friendship network among 28 financial elites. An edge indicates a friendship, and the network density is 0.168. We incorporate 13 binary node attributes detailing education (“Science Po”, “Polytechnique”, “Ecole Nationale d’Administration” [ENA]), career (“Inspection General de Finance” [IGF], “Cabinet”), social class (“Social Register”, “Father Status”, “particule”), political alignment (“Socialist”, “Capitalist”), and “Age”, which is associated with class in this context.

To determine the optimal number of latent dimensions, we compared the performance of our proposed COSS prior against standard model selection techniques by fitting the JLSM 100 times under various specifications. First, we employed our proposed approach, using the COSS prior with a truncation level of $k = 5$, allowing the effective dimension to be automatically inferred from $\{1, 2, 3, 4\}$. Second, we fitted the JLSM using a standard normal prior for the latent positions and selected the dimension based on AIC, BIC, 5-fold CV, and CV 1-SE rule (5-fold CV 1-SE). For the CV, the dimension was estimated by maximizing

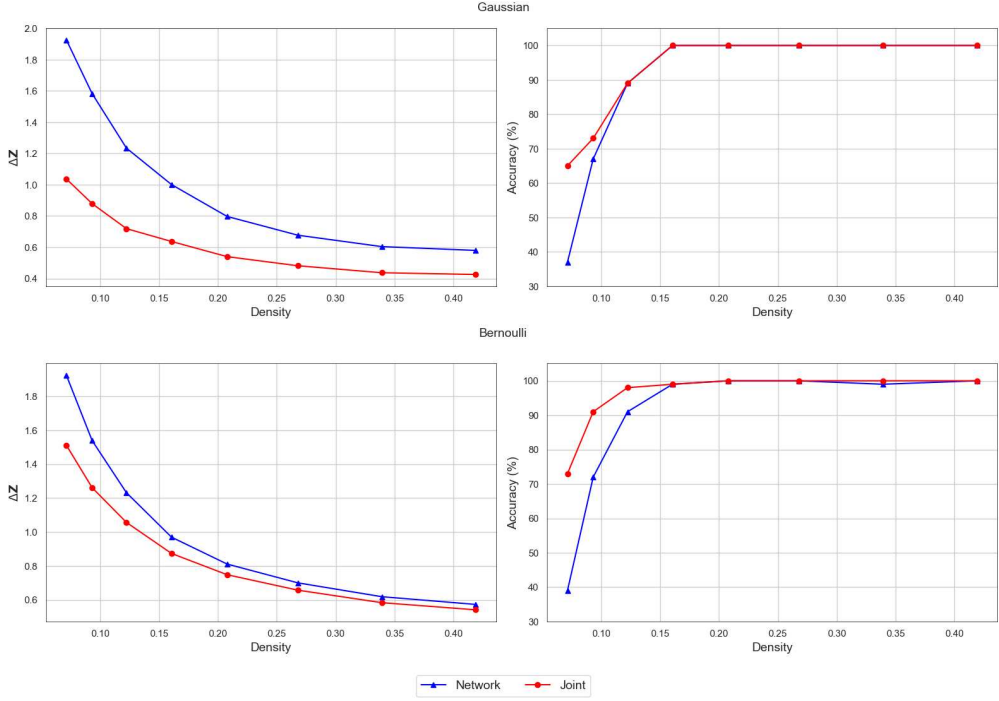


Figure 3: Latent structure estimation error (Δ_Z , left panels) and dimension recovery accuracy (%) versus network density for Gaussian (top) and Bernoulli (bottom) attributes.

the average held-out conditional likelihood.

Figure 4 summarizes the results. BIC consistently selects a one-dimensional space, likely due to its tendency to favor overly simple models in small samples. While CV frequently overestimates the dimension, favoring three dimensions. The proposed COSS prior, AIC, and K-fold CV 1-SE predominantly select two dimensions. Given the consistency across these methods and the known biases of BIC and standard CV in this context, we conclude that a two-dimensional latent space is most appropriate for this dataset.

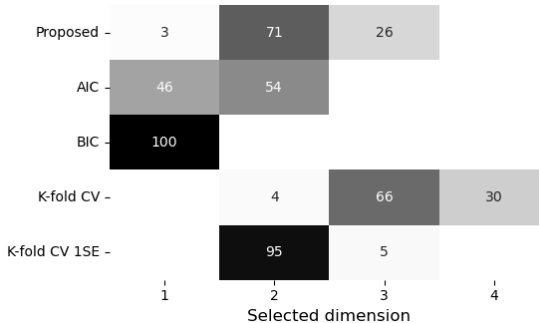


Figure 4: Estimated dimension for the French financial elites dataset. Darker cells indicate higher selection percentages.

Next, we interpret the two-dimensional latent space by examining the factor loadings and the visualization of the latent positions. Figure 5 presents a heatmap of the absolute values of the estimated loading matrix after a Geomin rotation (Yates, 1987). The loadings reveal a clear structure. The first dimension (F1) is strongly associated with attributes related to elite education and high-ranking career positions (ENA, IGF, Science Po, Polytechnique, Cabinet). The second dimension (F2) is characterized by indicators of established social class (Social Register, Father Status, particule) and older age. This aligns with the social divisions within the French elite described by Kadushin (1995).

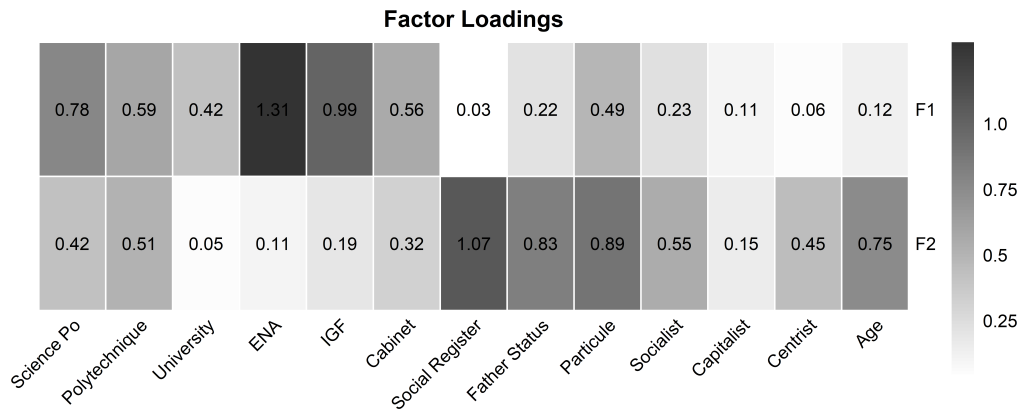


Figure 5: Heatmap of the estimated loading matrix \mathbf{B} in absolute value under Geomin rotation for the French financial elites dataset.

To further explore the estimated latent space, we visualize it in Figure 6. In the inner product latent space model, nodes with similar latent positions (i.e., those clustered together in the visualization) are more likely to form connections. We highlight ENA and Social Register, the attributes with the strongest loadings on the first and second dimensions, respectively. The left panel demonstrates a clear separation based on ENA affiliation. ENA graduates (purple nodes) form a cohesive, densely connected cluster (purple ellipse), distinct from the more dispersed non-ENA individuals (gray nodes). This reinforces the interpretation of the first dimension as representing educational attainment and the associated strong social ties formed in these institutions. The right panel highlights social class. Individuals listed in the Social Register (blue nodes) also cluster tightly (blue ellipse), indicating a strong tendency for connection among the established upper class. Our joint modeling approach provides quantitative support for the qualitative divisions previously identified, illustrating a social structure segmented by education and class.

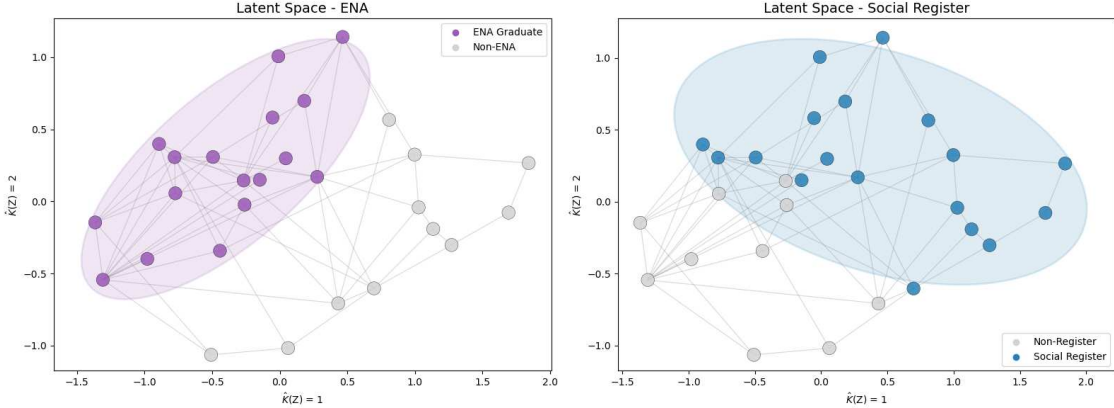


Figure 6: Latent Space Positioning of French Elites by ENA (Left Panel) and Social Register (Right Panel). Ellipses highlight the clustering of the respective groups.

7.2 Facebook Social Network Data

In this section, we evaluate our model’s performance on a missing data imputation task using data from Facebook ego network (Zhang et al., 2022)². The dataset comprises 10 ego-networks, where each network represents the connections among the friends of a specific user. The data include anonymized binary attributes for each user (e.g., an original attribute like “political = Democratic Party” is transformed into “political = anonymized feature 1”). We analyzed 8 of the 10 networks, excluding two that had too few nodes or highly sparse attribute vectors. We also removed attributes with extremely low or high prevalence within each network to ensure stable estimation as in Zhang et al. (2022). The goal is to impute missing attributes for a user based on their available profile information and their social connections.

In our experiment, we randomly masked 5% of the entries in the node attribute matrix \mathbf{Y} . We then imputed these missing values using both the network-only latent space model and our proposed joint latent space model. For the joint model, missing values were re-imputed as unknown parameters within each iteration of the Gibbs sampler. For the network-only model, we first estimated the latent positions \mathbf{Z}_{net} and then used these to predict the missing attributes by regressing \mathbf{Y} on \mathbf{Z}_{net} . As a benchmark, we also applied the Multiple Imputation by Chained Equations (MICE) method (Azur et al., 2011), a standard technique that utilizes only the node attributes.

Table 2 summarizes the prediction performance in terms of mean AUROC values and estimated latent dimensions \hat{K} over 30 replications. The results show that both network-based models outperform MICE across all networks, demonstrating that network structure

²The dataset is publicly available at <https://snap.stanford.edu/data/>

contains predictive information about node attributes that traditional attribute-only methods fail to capture. Furthermore, the joint latent space model consistently achieves the highest AUROC scores, indicating that there are meaningful associations between network features and node attributes, and that integrating them within a unified framework enhances predictive accuracy. As our simulation studies indicated, this ability to flexibly model the dimensionality does not detract from, but rather enhances, the model’s performance.

Finally, we find that the estimated latent dimension \hat{K} is higher in the joint model than in the network-only model. This suggests that the latent structures underlying the network and node attributes are not fully aligned. The joint model accommodates this misalignment by adding additional dimensions that primarily capture the node attribute information. As discussed in Section 2 and Zhang et al. (2022), this expanded latent space enables the model to represent both data sources effectively without sacrificing performance.

Table 2: Node variable imputation results for the Facebook dataset. Values reported are the mean AUROC and estimated dimensions \hat{K} across 30 replications.

Dataset	n	q	Density	\hat{K}		AUROC		
				Network	Joint	Network	Joint	MICE
Circle 1	347	56	0.042	4.68	5.43	0.845	0.904	0.801
Circle 2	547	58	0.030	5.22	6.93	0.857	0.921	0.853
Circle 3	227	87	0.124	6.00	7.53	0.820	0.875	0.716
Circle 4	159	55	0.134	3.00	6.20	0.804	0.866	0.740
Circle 5	170	37	0.155	5.13	6.70	0.791	0.869	0.779
Circle 6	792	100	0.049	8.53	9.57	0.872	0.931	0.853
Circle 7	755	66	0.105	8.01	9.80	0.868	0.918	0.874
Circle 8	1045	153	0.049	11.69	12.08	0.877	0.914	0.844

8 Conclusion

Network models in psychometrics increasingly integrate relational data with high-dimensional node attributes. While joint latent space models offer a powerful framework for this integration, their utility has been limited by the challenge of selecting the latent dimension, which typically relies on computationally intensive and sometimes unreliable post-hoc procedures. We introduced a novel, adaptive Bayesian JLSM that resolves this challenge by incorporating a non-homogeneous cumulative shrinkage spike-and-slab prior. This approach induces stochastic ordering and progressively shrinks superfluous dimensions, enabling automatic dimension selection simultaneously with parameter estimation within a unified inferential

framework.

The proposed methodology offers advantages across several aspects. First, we developed an efficient and scalable MCMC algorithm by leveraging a hierarchical representation of the prior and Pólya-Gamma data augmentation. Second, we established asymptotic guarantees for the proposed method, proving that the posterior concentrates on parsimonious models near the true dimension and achieves a near-optimal, adaptive Hellinger contraction rate for parameter estimation. Third, simulations confirmed that joint modeling improves estimation accuracy, especially with sparse networks. Furthermore, our adaptive approach outperforms standard dimension selection criteria. Applications to real data demonstrated the model’s utility in revealing latent social structures and enhancing predictive accuracy. A GitHub repository with documented code will be made publicly available upon acceptance of the paper.

This adaptive framework opens several avenues for future research. First, our model assumes that the network and node attributes arise from a single, fully shared latent space. While we have shown this is a reasonable and powerful approximation, future work could explore more flexible architectures that decompose the latent space into components that are shared versus specific to each data modality. Second, enhancing interpretability by addressing rotational invariance remains a promising direction. Although the shrinkage prior resolves column permutation invariance, further constraints such as structured sparsity priors on the loading matrix or the inclusion of relevant covariates could be incorporated to achieve an identifiable and interpretable latent structure. Finally, the methodology can be extended to accommodate more complex data structures common in psychometrics, including dynamic or directed weighted networks, and integrated with diverse psychometric models, such as the Generalized Partial Credit Model (GPCM).

Financial Support

The research was supported by the National Natural Science Foundation of China under Grant No.12301373, No.12271168, No.12271166, and No.12371289.

References

Azur, M. J., Stuart, E. A., Frangakis, C., and Leaf, P. J. (2011). Multiple imputation by chained equations: What is it and how does it work? *International Journal of Methods in Psychiatric Research*, 20(1):40–49.

Bhattacharya, A. and Dunson, D. B. (2011). Sparse Bayesian infinite factor models. *Biometrika*, 98(2):291–306.

Borsboom, D., Deserno, M. K., Rhemtulla, M., Epskamp, S., Fried, E. I., McNally, R. J., Robinaugh, D. J., Perugini, M., Dalege, J., Costantini, G., et al. (2021). Network analysis of multivariate data in psychological science. *Nature Reviews Methods Primers*, 1(1):58.

Che, C., Jin, I. H., and Zhang, Z. (2021). Network mediation analysis using model-based eigenvalue decomposition. *Structural Equation Modeling: A Multidisciplinary Journal*, 28(1):148–161.

Chen, K. and Lei, J. (2018). Network cross-validation for determining the number of communities in network data. *Journal of the American Statistical Association*, 113(521):241–251.

Durante, D. (2017). A note on the multiplicative gamma process. *Statistics & Probability Letters*, 122:198–204.

Durante, D. and Dunson, D. B. (2014). Nonparametric Bayes dynamic modelling of relational data. *Biometrika*, 101(4):883–898.

Epskamp, S., Borsboom, D., and Fried, E. I. (2018). Estimating psychological networks and their accuracy: A tutorial paper. *Behavior Research Methods*, 50(1):195–212.

Epskamp, S., Rhemtulla, M., and Borsboom, D. (2017). Generalized network psychometrics: Combining network and latent variable models. *Psychometrika*, 82(4):904–927.

Fratiglioni, L., Wang, H.-X., Ericsson, K., Maytan, M., and Winblad, B. (2000). Influence of social network on occurrence of dementia: A community-based longitudinal study. *The Lancet*, 355(9212):1315–1319.

Gollini, I. and Murphy, T. B. (2016). Joint modeling of multiple network views. *Journal of Computational and Graphical Statistics*, 25(1):246–265.

Guha, S. and Rodriguez, A. (2021). Bayesian regression with undirected network predictors with an application to brain connectome data. *Journal of the American Statistical Association*, 116(534):581–593.

Guhaniyogi, R. and Rodriguez, A. (2020). Joint modeling of longitudinal relational data and exogenous variables. *Bayesian Analysis*, 15(2):477–503.

Hoff, P. D. (2007). Modeling homophily and stochastic equivalence in symmetric relational data. *Advances in Neural Information Processing Systems*, 20:657–664.

Hoff, P. D., Raftery, A. E., and Handcock, M. S. (2002). Latent space approaches to social network analysis. *Journal of the American Statistical Association*, 97(460):1090–1098.

Ishwaran, H. and Rao, J. S. (2005). Spike and slab variable selection: Frequentist and Bayesian strategies. *The Annals of Statistics*, 33(2):730–773.

Jeon, M., Jin, I. H., Schweinberger, M., and Baugh, S. (2021). Mapping unobserved item–respondent interactions: A latent space item response model with interaction map. *Psychometrika*, 86(2):378–403.

Jin, I. H. and Jeon, M. (2019). A doubly latent space joint model for local item and person dependence in the analysis of item response data. *Psychometrika*, 84(1):236–260.

Kadushin, C. (1995). Friendship among the French financial elite. *American Sociological Review*, 60(2):202–221.

Legramanti, S., Durante, D., and Dunson, D. B. (2020). Bayesian cumulative shrinkage for infinite factorizations. *Biometrika*, 107(3):745–752.

Leskovec, J. and McAuley, J. (2012). Learning to discover social circles in ego networks. *Advances in Neural Information Processing Systems*, 25:539–547.

Li, J., Gibbons, R., and Ročková, V. (2025). Sparse Bayesian multidimensional item response theory. *Journal of the American Statistical Association*, pages 1–14.

Li, T., Levina, E., and Zhu, J. (2020). Network cross-validation by edge sampling. *Biometrika*, 107(2):257–276.

Liu, H., Jin, I. H., and Zhang, Z. (2018). Structural equation modeling of social networks: Specification, estimation, and application. *Multivariate Behavioral Research*, 53(5):714–730.

Liu, H., Jin, I. H., Zhang, Z., and Yuan, Y. (2021). Social network mediation analysis: A latent space approach. *Psychometrika*, 86(1):272–298.

Loyal, J. D. and Chen, Y. (2025). A spike-and-slab prior for dimension selection in generalized linear network eigenmodels. *Biometrika*, page asaf014.

Ma, Z., Ma, Z., and Yuan, H. (2020). Universal latent space model fitting for large networks with edge covariates. *Journal of Machine Learning Research*, 21(4):1–67.

Marsman, M., van den Bergh, D., and Haslbeck, J. M. B. (2025). Bayesian analysis of the ordinal Markov random field. *Psychometrika*, 90(1):146–182.

McCallum, A. K., Nigam, K., Rennie, J., and Seymore, K. (2000). Automating the construction of internet portals with machine learning. *Information Retrieval*, 3:127–163.

McPherson, M., Smith-Lovin, L., and Cook, J. M. (2001). Birds of a feather: Homophily in social networks. *Annual Review of Sociology*, 27(1):415–444.

Polson, N. G., Scott, J. G., and Windle, J. (2013). Bayesian inference for logistic models using Pólya–Gamma latent variables. *Journal of the American Statistical Association*, 108(504):1339–1349.

Roberts, G. O. and Rosenthal, J. S. (2007). Coupling and ergodicity of adaptive Markov chain Monte Carlo algorithms. *Journal of Applied Probability*, 44(2):458–475.

Ročková, V. and George, E. I. (2016). Fast Bayesian factor analysis via automatic rotations to sparsity. *Journal of the American Statistical Association*, 111(516):1608–1622.

Salter-Townshend, M. and McCormick, T. H. (2017). Latent space models for multiview network data. *The Annals of Applied Statistics*, 11(3):1217–1244.

Schiavon, L., Canale, A., and Dunson, D. B. (2022). Generalized infinite factorization models. *Biometrika*, 109(3):817–835.

Shalizi, C. R. and Thomas, A. C. (2011). Homophily and contagion are generically confounded in observational social network studies. *Sociological Methods & Research*, 40(2):211–239.

Spiegelhalter, D. J., Best, N. G., Carlin, B. P., and van der Linde, A. (2002). Bayesian measures of model complexity and fit. *Journal of the Royal Statistical Society: Series B (Statistical Methodology)*, 64(4):583–639.

Sweet, T. and Adhikari, S. (2020). A latent space network model for social influence. *Psychometrika*, 85(2):251–274.

Sweet, T. M. (2015). Incorporating covariates into stochastic blockmodels. *Journal of Educational and Behavioral Statistics*, 40(6):635–664.

Sweet, T. M. (2016). Social network methods for the educational and psychological sciences. *Educational psychologist*, 51(3-4):381–394.

Vaida, F. and Blanchard, S. (2005). Conditional Akaike information for mixed-effects models. *Biometrika*, 92(2):351–370.

VanderWeele, T. J. (2011). Sensitivity analysis for contagion effects in social networks. *Sociological methods & research*, 40(2):240–255.

Wang, S. (2021). Recent integrations of latent variable network modeling with psychometric models. *Frontiers in Psychology*, 12:773289.

Wang, S., Paul, S., and De Boeck, P. (2023). Joint latent space model for social networks with multivariate attributes. *psychometrika*, 88(4):1197–1227.

Xie, F. and Xu, Y. (2020). Optimal Bayesian estimation for random dot product graphs. *Biometrika*, 107(4):875–889.

Yates, A. (1987). *Multivariate Exploratory Data Analysis: A Perspective on Exploratory Factor Analysis*. SUNY Press, Albany, NY.

Zhang, X., Xu, G., and Zhu, J. (2022). Joint latent space models for network data with high-dimensional node variables. *Biometrika*, 109(3):707–720.

Zhang, Y., Levina, E., and Zhu, J. (2016). Community detection in networks with node features. *Electronic Journal of Statistics*, 10(2):3153–3178.

Supplementary materials for “Adaptive Bayesian Joint Latent Space Modeling via Cumulative Shrinkage”

Bin Lv, Yincai Tang, and Siliang Zhang*

Key Laboratory of Advanced Theory and Application in Statistics and Data Science-MOE, School of Statistics, East China Normal University

Contents

Appendix A Computational Details	1
A.1 Gibbs Sampler for JLSM with Gaussian Node Attributes	1
A.2 Gibbs Sampler for JLSM with Bernoulli Node Attributes	3
A.3 Definitions of competing model selection criteria	5
Appendix B Theoretical Details and Proofs	5
B.1 Preliminaries	5
B.1.1 Notations and Regularity Conditions	5
B.1.2 Definition of the Hellinger Metric	6
B.2 Proof of Prior Properties (Proposition 1 and Corollary 1)	7
B.3 Proofs of Main Asymptotic Results	7
B.3.1 Technical Lemmas	7
B.3.2 Proof of Theorem 1 (Posterior Concentration for the Latent Dimension)	13
B.3.3 Proof of Theorem 2 (Posterior Contraction Rate)	14
B.4 Corollary on Frobenius Norm Convergence	19

Appendix A Computational Details

A.1 Gibbs Sampler for JLSM with Gaussian Node Attributes

Algorithm 1. One cycle of the Gibbs sampler for joint latent space model with the cumulative ordered spike-and-slab prior.

Step. 1: For $i = 1$ to n and $i' = 1$ to $i - 1$, sample augmented data $d_{ii'}^A$ from the full conditional

*Corresponding author: slzhang@fem.ecnu.edu.cn

Pólya-Gamma distribution:

$$d_{ii'}^A \mid \text{rest} = d_{i'i}^A \mid \text{rest} \sim \text{PG}(1, \Theta_{ii'}^A).$$

Step. 2: For $i = 1$ to n , sample α_i from its conditional normal distribution:

$$\alpha_i \mid \text{rest} \sim \mathcal{N} \left(\sigma_{\alpha_i}^2 \sum_{i' \neq i} \{A_{ii'} - 1/2 - d_{ii'}^A(\alpha_{i'} + \mathbf{z}_{i'}^\top \mathbf{z}_{i'})\}, \sigma_{\alpha_i}^2 \right), \quad (\text{S1})$$

where $\sigma_{\alpha_i}^2 = 1 / \left(\sum_{i' \neq i} d_{ii'}^A + \sigma_\alpha^{-2} \right)$.

Step. 3: For $i = 1$ to n , sample \mathbf{z}_i from its conditional normal distribution given $\mathbf{Z}^{(-i)}$ and $\boldsymbol{\alpha}^{(-i')}$, where $\mathbf{Z}^{(-i)} = [\mathbf{z}_1, \dots, \mathbf{z}_{i-1}, \mathbf{z}_{i+1}, \dots, \mathbf{z}_n]^\top$, $\boldsymbol{\alpha}^{(-i')} = (\alpha_1 + \alpha_i, \dots, \alpha_{i-1} + \alpha_i, \alpha_{i+1} + \alpha_i, \dots, \alpha_n + \alpha_i)^\top$,

$$\mathbf{z}_i \mid \text{rest} \sim \mathcal{N}(\mu_{\mathbf{z}_i}, \Sigma_{\mathbf{z}_i}), \quad (\text{S2})$$

where

$$\begin{aligned} \Sigma_{\mathbf{z}_i} &= \left(\mathbf{Z}^{(-i)\top} \mathbf{D}_A^{(-i)} \mathbf{Z}^{(-i)} + \mathbf{B}^\top \Sigma_Y^{-1} \mathbf{B} + \Sigma_Z^{-1} \right)^{-1}, \\ \mu_{\mathbf{z}_i} &= \Sigma_{\mathbf{z}_i} \left(\mathbf{Z}^{(-i)\top} (\boldsymbol{\kappa}_{A^{(-i)}} - \mathbf{D}_A^{(-i)} \boldsymbol{\alpha}^{(-i')}) + \mathbf{B}^\top \Sigma_Y^{-1} (\mathbf{y}_i - \boldsymbol{\gamma}) \right), \end{aligned}$$

with $\mathbf{D}_A^{(-i)} = \text{diag}(d_{i1}^A, \dots, d_{i,i-1}^A, d_{i,i+1}^A, \dots, d_{in}^A)$, $\Sigma_Z = \text{diag}(\theta_1, \dots, \theta_k)$, $\Sigma_Y = \text{diag}(\sigma_1^2, \dots, \sigma_q^2)$, $\boldsymbol{\kappa}_{A^{(-i)}} = (A_{i1} - \frac{1}{2}, \dots, A_{i,i-1} - \frac{1}{2}, A_{i,i+1} - \frac{1}{2}, \dots, A_{in} - \frac{1}{2})^\top$.

Step. 4: Sample $\boldsymbol{\gamma}$ from its conditional normal distribution:

$$\boldsymbol{\gamma} \mid \text{rest} \sim \mathcal{N} \left(\Sigma_\gamma \begin{bmatrix} \sigma_1^{-2} \sum_{i=1}^n \{Y_{i1} - \mathbf{z}_i^\top \boldsymbol{\beta}_1\} \\ \vdots \\ \sigma_q^{-2} \sum_{i=1}^n \{Y_{in} - \mathbf{z}_i^\top \boldsymbol{\beta}_q\} \end{bmatrix}, \Sigma_\gamma \right), \quad (\text{S3})$$

where $\Sigma_\gamma = \text{diag} \left(\frac{\sigma_\gamma^2 \sigma_1^2}{n\sigma_\gamma^2 + \sigma_1^2}, \dots, \frac{\sigma_\gamma^2 \sigma_q^2}{n\sigma_\gamma^2 + \sigma_q^2} \right)$.

Step. 5: For each $j = 1$ to q , sample the j -th column $\boldsymbol{\beta}_j$ of \mathbf{B} from its conditional normal distribution:

$$\boldsymbol{\beta}_j \mid \text{rest} \sim \mathcal{N}((\mathbf{I}_k + \sigma_j^{-2} \mathbf{Z}^\top \mathbf{Z})^{-1} \mathbf{Z}^\top \sigma_j^{-2} (\mathbf{Y}_{\cdot j} - \gamma_j \mathbf{1}_n), (\mathbf{I}_k + \sigma_j^{-2} \mathbf{Z}^\top \mathbf{Z})^{-1}).$$

Step. 6: For each $j = 1$ to q , sample the variance parameter σ_j^2 from its conditional inverse gamma distribution:

$$\sigma_j^2 \mid \text{rest} \sim \text{IG} \left(a_\sigma + \frac{n}{2}, b_\sigma + \frac{1}{2} \|\mathbf{Y}_{\cdot j} - \gamma_j \mathbf{1}_n - \mathbf{Z} \boldsymbol{\beta}_j\|_2^2 \right).$$

Step. 7: For $h = 1$ to k , sample the indicator variables ρ_h from their conditional distribution:

$$\Pr(\rho_h = l \mid \text{rest}) \propto \begin{cases} \omega_l \mathcal{N}(\mathbf{Z}_{\cdot h}; 0, \theta_0 \mathbf{I}_n), & l = 1, \dots, h, \\ \omega_l t_{2a_\theta}(\mathbf{Z}_{\cdot h}; 0, (a_\theta/b_\theta) \mathbf{I}_n), & l = h + 1, \dots, k. \end{cases}$$

Step. 8: Sample v_1 from its conditional Beta distribution:

$$v_1 \mid \text{rest} \sim \text{Beta} \left(\kappa + \sum_{j=1}^k \mathbb{1}(\rho_j = 1), 1 + \sum_{j=1}^k \mathbb{1}(\rho_j > 1) \right).$$

Step. 9: For $h = 2$ to $k - 1$, sample v_h from its conditional Beta distribution:

$$v_h \mid \text{rest} \sim \text{Beta} \left(a + \sum_{j=1}^k \mathbb{1}(\rho_j = h), 1 + \sum_{j=1}^k \mathbb{1}(\rho_j > h) \right).$$

Set $v_k = 1$ and compute $\omega_1, \dots, \omega_k$ according to Eq. (7).

Step. 10: For $h = 1$ to k , if $\rho_h \leq h$, set $\theta_h = \theta_0$. Otherwise, sample θ_h from its conditional inverse gamma distribution:

$$\theta_h \mid \text{rest} \sim \text{IG} \left(a_\theta + \frac{n}{2}, b_\theta + \frac{1}{2} \|\mathbf{Z}_{\cdot, h}\|_2^2 \right).$$

A.2 Gibbs Sampler for JLSM with Bernoulli Node Attributes

We can easily obtain the Gibbs sampler when node variables \mathbf{Y} satisfy the MIRT model by further introducing augmentation data d_{ij}^Y .

Algorithm 2. One cycle of the Gibbs sampler for joint latent space model with the cumulative ordered spike-and-slab prior.

Step. 1: For $i = 1$ to n and $i' = 1$ to $i - 1$, sample augmented data $d_{ii'}^A$ from the full conditional Pólya-Gamma distribution:

$$d_{ii'}^A \mid \text{rest} = d_{i'i}^A \mid \text{rest} \sim \text{PG}(1, \Theta_{ii'}^A).$$

Step. 2: For $i = 1$ to n and $j = 1$ to q , sample augmented data d_{ij}^Y from the full conditional Pólya-Gamma distribution:

$$d_{ij}^Y \mid \text{rest} \sim \text{PG}(1, \Theta_{ij}^Y).$$

Step. 3: For $i = 1$ to n , sample α_i from its conditional normal distribution:

$$\alpha_i \mid \text{rest} \sim \mathcal{N} \left(\sigma_{\alpha_i}^2 \sum_{i' \neq i} \{A_{ii'} - 1/2 - d_{ii'}^A(\alpha_{i'} + \mathbf{z}_i^\top \mathbf{z}_{i'})\}, \sigma_{\alpha_i}^2 \right),$$

where $\sigma_{\alpha_i}^2 = 1 / \left(\sum_{i' \neq i} d_{ii'}^A + \sigma_\alpha^{-2} \right)$.

Step. 4: For $i = 1$ to n , sample \mathbf{z}_i from its conditional normal distribution given $\mathbf{Z}^{(-i)}$ and $\boldsymbol{\alpha}^{(-i')}$, where $\mathbf{Z}^{(-i)} = [\mathbf{z}_1, \dots, \mathbf{z}_{i-1}, \mathbf{z}_{i+1}, \dots, \mathbf{z}_n]^\top$, $\boldsymbol{\alpha}^{(-i')} = (\alpha_1 + \alpha_i, \dots, \alpha_{i-1} + \alpha_i, \alpha_{i+1} + \alpha_i, \dots, \alpha_n + \alpha_i)^\top$,

$$\mathbf{z}_i \mid \text{rest} \sim \mathcal{N}(\mu_{\mathbf{z}_i}, \Sigma_{\mathbf{z}_i}),$$

where

$$\begin{aligned}\Sigma_{\mathbf{z}_i} &= (\mathbf{Z}^{(-i)\top} \mathbf{D}_A^{(-i)} \mathbf{Z}^{(-i)} + \mathbf{B}^\top \mathbf{D}_Y^{(i)} \mathbf{B} + \Sigma_Z^{-1})^{-1}, \\ \mu_{\mathbf{z}_i} &= \Sigma_{\mathbf{z}_i} (\mathbf{Z}^{(-i)\top} (\boldsymbol{\kappa}_{A^{(-i)}} - \mathbf{D}_A^{(-i)} \boldsymbol{\alpha}^{(-i')}) + \mathbf{B}^\top (\boldsymbol{\kappa}_{Y^{(i)}} - \mathbf{D}_Y^{(i)} \boldsymbol{\gamma})),\end{aligned}$$

with $\mathbf{D}_A^{(-i)} = \text{diag}(d_{i1}^A, \dots, d_{i,i-1}^A, d_{i,i+1}^A, \dots, d_{in}^A)$, $\mathbf{D}_Y^{(i)} = \text{diag}(d_{i1}^Y, \dots, d_{iq}^Y)$, $\Sigma_Z = \text{diag}(\theta_1, \dots, \theta_k)$, $\boldsymbol{\kappa}_{A^{(-i)}} = (A_{i1} - \frac{1}{2}, \dots, A_{i,i-1} - \frac{1}{2}, A_{i,i+1} - \frac{1}{2}, \dots, A_{in} - \frac{1}{2})^\top$ and $\boldsymbol{\kappa}_{Y^{(i)}} = (Y_{i1} - \frac{1}{2}, \dots, Y_{iq} - \frac{1}{2})^\top$.

Step. 5: Sample $\boldsymbol{\gamma}$ from its conditional normal distribution:

$$\boldsymbol{\gamma} | \text{rest} \sim \mathcal{N} \left(\Sigma_\gamma \begin{bmatrix} \sum_{i=1}^n \{Y_{i1} - \frac{1}{2} - d_{i1}^Y \mathbf{z}_i^\top \boldsymbol{\beta}_1\} \\ \vdots \\ \sum_{i=1}^n \{Y_{in} - \frac{1}{2} - d_{iq}^Y \mathbf{z}_i^\top \boldsymbol{\beta}_q\} \end{bmatrix}, \Sigma_\gamma \right)$$

where $\Sigma_\gamma = (\text{diag}(\sum_{i=1}^n d_{i1}^Y, \dots, \sum_{i=1}^n d_{iq}^Y) + \sigma_\gamma^{-2} \mathbf{I}_q)^{-1}$.

Step. 6: For each $j = 1$ to q , sample the j -th column $\boldsymbol{\beta}_j$ of \mathbf{B} from its conditional normal distribution:

$$\boldsymbol{\beta}_j | \text{rest} \sim \mathcal{N}((\mathbf{I}_k + \mathbf{Z}^\top \mathbf{D}_Y^{(j)'} \mathbf{Z})^{-1} \mathbf{Z}^\top (\boldsymbol{\kappa}_{Y^{(j)'}} - \mathbf{D}_Y^{(j)'} \boldsymbol{\gamma} \mathbf{1}_n), (\mathbf{I}_k + \mathbf{Z}^\top \mathbf{D}_Y^{(j)'} \mathbf{Z})^{-1}),$$

where $\mathbf{D}_Y^{(j)'} = \text{diag}(d_{1j}^Y, \dots, d_{nj}^Y)$, $\boldsymbol{\kappa}_{Y^{(j)'}} = (Y_{1j} - \frac{1}{2}, \dots, Y_{nj} - \frac{1}{2})^\top$.

Step. 7: For $h = 1$ to k , sample the indicator variables ρ_h from their conditional distribution:

$$\Pr(\rho_h = l | \text{rest}) \propto \begin{cases} \omega_l \mathcal{N}(\mathbf{Z}_{\cdot h}; 0, \theta_0 \mathbf{I}_n), & l = 1, \dots, h, \\ \omega_l t_{2a_\theta}(\mathbf{Z}_{\cdot h}; 0, (a_\theta/b_\theta) \mathbf{I}_n), & l = h+1, \dots, k. \end{cases}$$

Step. 8: Sample v_1 from its conditional Beta distribution:

$$v_1 | \text{rest} \sim \text{Beta} \left(\kappa + \sum_{j=1}^k \mathbb{1}(\rho_j = 1), 1 + \sum_{j=1}^k \mathbb{1}(\rho_j > 1) \right).$$

Step. 9: For $h = 2$ to $k-1$, sample v_h from its conditional Beta distribution:

$$v_h | \text{rest} \sim \text{Beta} \left(a + \sum_{j=1}^k \mathbb{1}(\rho_j = h), 1 + \sum_{j=1}^k \mathbb{1}(\rho_j > h) \right).$$

Set $v_k = 1$ and compute $\omega_1, \dots, \omega_k$ according to Eq. (7).

Step. 10: For $h = 1$ to k , if $\rho_h \leq h$, set $\theta_h = \theta_0$. Otherwise, sample θ_h from its conditional inverse gamma distribution:

$$\theta_h | \text{rest} \sim \text{IG} \left(a_\theta + \frac{n}{2}, b_\theta + \frac{1}{2} \|\mathbf{Z}_{\cdot h}\|_2^2 \right).$$

A.3 Definitions of competing model selection criteria

Let $\{\xi^{(s)}\}_{s=1}^S$ denote the S posterior samples from the Bayesian model under consideration. In addition, $\hat{\xi}$ denote the posterior mean of the parameters based on these posterior samples. Then the AIC is defined as

$$\text{AIC} = -2 \log \Pr(A, Y | \hat{\xi}) + 2d,$$

where d is the number of the parameters, that is, $nk + qk + n + 2q$ for gaussian node variables and $nk + qk + n + q$ for bernoulli node variables. Similarly, the BIC is defined as

$$\text{BIC} = -2 \log \Pr(A, Y | \hat{\xi}) + 2d \log n,$$

where d is same as in the AIC. The DIC is defined as

$$\text{DIC} = -2 \log \Pr(A, Y | \hat{\xi}) + 2p_{\text{DIC}},$$

where $p_{\text{DIC}} = 2 \left(\log \Pr(A, Y | \hat{\xi}) - \frac{1}{S} \sum_{s=1}^S \log \Pr(A, Y | \xi^{(s)}) \right)$. The WAIC is defined as

$$\begin{aligned} \text{WAIC} = & -2 \left(\sum_{i=1}^n \sum_{i'=1}^{i-1} \log \left(\frac{1}{S} \sum_{s=1}^S \Pr(A_{ii'} | \xi^{(s)}) \right) + \sum_{i=1}^n \sum_{j=1}^q \log \left(\frac{1}{S} \sum_{s=1}^S \Pr(Y_{ij} | \xi^{(s)}) \right) \right. \\ & \left. - \sum_{i=1}^n \sum_{i'=1}^{i-1} \text{Var}(\log \Pr(A_{ii'} | \xi)) - \sum_{i=1}^n \sum_{j=1}^q \text{Var}(\log \Pr(Y_{ij} | \xi)) \right), \end{aligned}$$

where $\text{Var}(\log \Pr(A_{ii'} | \xi))$ and $\text{Var}(\log \Pr(Y_{ij} | \xi))$ denote the sample variance of the log-likelihood evaluated over the posterior samples $\{\xi^{(s)}\}_{s=1}^S$. Lastly, we considered the K-fold cross-validation as follows:

- We randomly divide the nodes in the $n \times n$ adjacency matrix A and $n \times q$ node variables Y into K equal sizes, using one set of data points as the test data and other sets of data points as the training data.
- For each $k \in \{1, \dots, K\}$, we fit the training data to JLSM with the number of dimensions equaling to k . We obtain the posterior mean of the model parameters and use them as parameters to obtain predictions for the test data.
- Based on the observed test data and the predicted probabilities for the test data, we obtain the held-out log-likelihood.

Appendix B Theoretical Details and Proofs

B.1 Preliminaries

B.1.1 Notations and Regularity Conditions

Let $\{a_n\}$ and $\{b_n\}$ be two sequences of positive numbers.

- We write $a_n \lesssim b_n$ or $b_n \gtrsim a_n$ if there exists a constant $C > 0$ such that $a_n \leq Cb_n$ for all sufficiently large n .
- We write $a_n \asymp b_n$ if $a_n \lesssim b_n$ and $a_n \gtrsim b_n$.
- For a real number x , $\lceil x \rceil$ denotes the smallest integer greater than or equal to x , and $\lfloor x \rfloor$ denotes the largest integer less than or equal to x .

Our main theoretical results rely on the following conditions regarding the growth of the model and the properties of the true data-generating process.

Assumption S1 (Growth Conditions). *The truncation level k , the number of attributes q , and the true dimension k_0 satisfy:*

- (a) $k = \lceil n^\lambda \rceil$ for some constant $\lambda \in (0, 1]$.
- (b) $q \lesssim n$.
- (c) $k_0 / \log k \rightarrow 0$ as $n \rightarrow \infty$.

Assumption S2 (Boundedness of True Parameters). *There exist positive constants $C_\alpha, C_\gamma, C_Z, C'_Z, C_B, C'_B$ such that the true parameters satisfy:*

- (a) (Heterogeneity) $\max_{1 \leq i \leq n} |\alpha_{0,i}| \leq C_\alpha$.
- (b) (Intercepts) $\max_{1 \leq j \leq q} |\gamma_{0,j}| \leq C_\gamma$.
- (c) (Latent Positions) $\max_{i,h} |z_{0,ih}| \leq C_Z$ and $\max_{i,i'} |\mathbf{z}_{0,i}^\top \mathbf{z}_{0,i'}| \leq C'_Z$.
- (d) (Loadings) $\max_{j,h} |\beta_{0,jh}| \leq C_B$ and $\max_{i,j} |\mathbf{z}_{0,i}^\top \boldsymbol{\beta}_{0,j}| \leq C'_B$.

Assumption S3 (Regularity of the GLM Component). *The function $f_Y(\cdot)$ from the exponential family formulation of the node attribute model satisfies:*

- (a) (Bounded Variance) For any compact set $\mathcal{K} \subset \mathbb{R}$, there exists a constant C_f such that $\sup_{\Theta \in \mathcal{K}} f_Y''(\Theta) \leq C_f$.
- (b) (Polynomial Tail Growth) Define $\psi_Y(L) = 1 + \sup_{|x| \leq L(1+2L)} f_Y''(x)$. For any constants $M_1, M_2 > 0$, we have $\log \psi_Y(M_1 n^{M_2}) \lesssim \log n$. This is satisfied by Gaussian and Bernoulli (logit/probit link) models.

B.1.2 Definition of the Hellinger Metric

Let $\boldsymbol{\Theta} = \{\boldsymbol{\alpha}, \boldsymbol{\gamma}, \mathbf{Z}, \mathbf{B}\}$ be a collection of parameters. The model implies marginal densities $p_{\Theta_{ii'}^A}$ for each edge variable $A_{ii'}$ and $p_{\Theta_{ij}^Y}$ for each node attribute Y_{ij} . For two parameter sets $\boldsymbol{\Theta}_1$ and $\boldsymbol{\Theta}_2$, the root-averaged-squared Hellinger metric is defined as:

$$H_n(\boldsymbol{\Theta}_1, \boldsymbol{\Theta}_2) = \left[\frac{2}{n(n+2q-1)} \left(\sum_{i=1}^n \sum_{i'=1}^{i-1} h^2(p_{\Theta_{1,ii'}^A}, p_{\Theta_{2,ii'}^A}) + \sum_{i=1}^n \sum_{j=1}^q h^2(p_{\Theta_{1,ij}^Y}, p_{\Theta_{2,ij}^Y}) \right) \right]^{1/2}, \quad (\text{S4})$$

where $h^2(p_1, p_2) = \int (\sqrt{p_1(x)} - \sqrt{p_2(x)})^2 dx$ is the squared Hellinger distance between two densities p_1 and p_2 .

B.2 Proof of Prior Properties (Proposition 1 and Corollary 1)

Proof of proposition 1. The proof proceeds directly:

$$\Pr(|\theta_h| > \epsilon) = \mathbb{E}[\Pr(|\theta_h| > \epsilon | \pi_h)] = \mathbb{E}(1 - \pi_h)P_{\text{slab}}(|\theta_h| > \epsilon).$$

Since $\mathbb{E}(1 - \pi_h) = \frac{1}{\kappa+1} \left(\frac{1}{a+1} \right)^{h-1}$, $(1 \leq h \leq k-1)$ is decreasing in h and $\pi_k = 1$, the result follows. \square

Proof of corollary 1. The proof proceeds directly:

$$\Pr(|z_{ih}| \leq \epsilon) = \mathbb{E}[\Pr(|z_{ih}| \leq \epsilon | \pi_h)] = \mathbb{E}(1 - \pi_h)P_{\text{slab}}(|z_{ih}| \leq \epsilon) + \mathbb{E}(\pi_h)P_{\text{spike}}(|z_{ih}| \leq \epsilon).$$

Since $P_{\text{slab}}(|z_{ih}| \leq \epsilon) > P_{\text{spike}}(|z_{ih}| \leq \epsilon)$ if $b_\theta/a_\theta > \theta_0$ where $P_{\text{spike}} = t_{2a_\theta}(0, b_\theta/a_\theta)$ and $P_{\text{spike}} = \mathcal{N}(0, \theta_0)$, the result follows. \square

B.3 Proofs of Main Asymptotic Results

B.3.1 Technical Lemmas

Outline of proofs The proofs of Theorems 1 and 2 follow the general framework for posterior concentration developed by Ghosal and van der Vaart (2007) and adapted for sparse generalized linear models by Jeong and Ghosal (2020). The main steps are as follows:

1. We first show that the prior distribution assigns sufficient mass to a shrinking Kullback-Leibler (KL) neighborhood around the true parameter value Θ_0 . This involves constructing a specific element in the support of the prior that is close to the truth and leveraging the properties of the cumulative shrinkage process.
2. We define a sequence of subsets of the parameter space, called a “sieve,” indexed by the number of active latent dimensions. Lemma S3 is critical for showing that the prior probability of parameter sets outside these sieves decays exponentially, allowing us to control the model complexity.
3. For any two parameter sets Θ_1 and Θ_2 , we construct uniformly consistent statistical tests to distinguish between them. The power of these tests depends on the Hellinger distance $H_n(\Theta_1, \Theta_2)$.
4. By combining these three components, the general theory guarantees that the posterior probability of the parameter space outside a Hellinger ball of radius ϵ_n around the true value Θ_0 converges to zero in probability. Theorem 1 is obtained as an intermediate result in this process, where the posterior mass is shown to concentrate on the sieve corresponding to the true dimension k_0 .

The remaining results analyze properties of the posterior distribution. When possible, we will prove the results for a general fractional posterior to simplify the proofs of parameter consistency in Section 5.

As in Jeong and Ghosal (2020), we write the fractional posterior as

$$\Pr(\mathcal{B} \mid \mathbf{A}, \mathbf{Y}) = \frac{N_n(\mathcal{B})}{D_n},$$

where

$$N_n(\mathcal{B}) = \int_{\mathcal{B}} \prod_{i < i'} \frac{p_{\Theta_{ii'}^A}(A_{ii'})}{p_{\Theta_{0ii'}^A}(A_{ii'})} \prod_{i,j} \frac{p_{\Theta_{ij}^Y}(Y_{ij})}{p_{\Theta_{0ij}^Y}(Y_{ij})} d\Pi(\boldsymbol{\alpha}) d\Pi(\boldsymbol{\gamma}) d\Pi(\mathbf{Z}) d\Pi(\mathbf{B}), \quad (\text{S5})$$

$$D_n = N_n(\mathbb{R}^n \times \mathbb{R}^q \times \mathbb{R}^{n \times k} \times \mathbb{R}^{q \times k}), \quad (\text{S6})$$

for any measurable set $\mathcal{B} \subset \mathbb{R}^n \times \mathbb{R}^q \times \mathbb{R}^{n \times k} \times \mathbb{R}^{q \times k}$ and prior distributions $\Pi(\boldsymbol{\alpha})$, $\Pi(\boldsymbol{\gamma})$, $\Pi(\mathbf{Z})$ and $\Pi(\mathbf{B})$ for $\boldsymbol{\alpha}$, $\boldsymbol{\gamma}$, \mathbf{Z} and \mathbf{B} respectively. Before proving Theorem 1 and Theorem 2, we need the following lemmas.

Lemma S1. (Boucheron et al. (2013); Ning et al. (2020)) Let $X \sim \Gamma(a, b)$ and $h_1(u) = 1 + u - \sqrt{1 + 2u}$ for $u > 0$. For every $t > 0$, we have

$$\Pr(X > t) \leq \exp \left\{ -ah_1 \left(\frac{t}{ab} \right) \right\} \leq \exp \left(-\frac{t}{2b} + a \right).$$

Lemma S2. (Lemma S6 of Loyal and Chen (2025)) Let X_1, \dots, X_n be independent Bernoulli random variables with $\Pr(X_i = 1) = p_i$ for $i = 1, \dots, n$, such that $p_1 > p_2 > \dots > p_n$. Let $S_n = \sum_{i=1}^n X_i$ and $p = \sum_{i=1}^n p_i$, then

$$\Pr(S_n > an) \leq \left\{ \left(\frac{p_1}{a} \right)^a e^a \right\}^n,$$

for $p_1 \leq a < 1$.

Lemma S3 (Prior Concentration on Sparsity). Let $\boldsymbol{\theta} = (\theta_1, \dots, \theta_k)$ follow the prior defined by (5)–(6) with $P_{\text{spike}} = \delta_0$. If the hyperparameters are set such that $\kappa = k^{1+\delta}$ with $\delta > 6/\log k$, then for any $t \geq 1$:

$$\Pr(\|\boldsymbol{\theta}\|_0 > t) \leq 2e^{-t(\delta/6)\log k}.$$

where $\|\boldsymbol{\theta}\|_0 = \sum_{h=1}^k \mathbb{1}(\theta_h \neq 0)$ is the number of active (non-zero variance) dimensions.

proof of lemma S3. Since the inequality follows trivially when $t \geq k$, we assume $t < k$. Defined the random variable $S_k = \sum_{h=1}^k \mathbb{1}\{\theta_h \neq 0\}$. We bounded $\Pr(S_k > t)$ as follows:

$$\Pr(S_k > t) \leq \mathbb{E} \left\{ \Pr(S_k > t \mid \{\pi_h\}_{h=1}^k) \mathbb{1}\{\pi_1 > 1 - \tilde{\pi}\} \right\} + \Pr(\pi_1 \leq 1 - \tilde{\pi}),$$

where $\tilde{\pi} = t\delta \log k / 6k^{1+\delta}$. Condition on $\{\pi_h\}_{h=1}^k$, S_k is sum of independent Bernoulli random variables with success probabilities

$$p_h = \Pr(\theta_h \neq 0) = 1 - \pi_h,$$

with the property $p_1 > p_2 > \dots > p_k$ by construction. In addition, on the event $\{\pi_1 > 1 - \tilde{\pi}\}$, we have $p_1 = 1 - \pi_1 < t\delta \log k / 6k^{1+\delta} = (t/6k)\delta \log k \exp(-\delta \log k) < t/k < 1$, where we use the fact that

$e^{-x} < 1/x$ for $x > 0$. As we apply Lemma S2 to bound $\Pr(S_k > t \mid \{\pi_h\}_{h=1}^k)$, we have

$$\begin{aligned}
\Pr(S_k > t \mid \{\pi_h\}_{h=1}^k) &= \Pr\left(S_k > \frac{t}{k}k \mid \{\pi_h\}_{h=1}^k\right) \\
&\leq \left\{ \left((1 - \pi_1) \frac{k}{t} \right)^{t/k} e^{t/k} \right\}^k \\
&\leq \left(\frac{t\delta \log k}{6k^{1+\delta}} \frac{k}{t} \right)^t e^t \\
&= \left(\frac{\log k^{\delta/2}}{3k^\delta} \right)^t e^t \\
&\leq \left(\frac{1}{3k^{\delta/2}} \right)^t \\
&\leq e^{-t(\delta/2) \log k},
\end{aligned}$$

where we use the fact that $\log x < (1/e)x$ for any $x > 0$ in fifth line.

Now, we bound $\Pr(\pi_1 \leq 1 - \tilde{\pi}) = \Pr(v_1 \leq 1 - \tilde{\pi})$, where $v_1 \sim \text{Beta}(k^{1+\delta}, 1)$. Then, we have,

$$\begin{aligned}
\Pr(v_1 \geq \tilde{\pi}) &= k^{1+\delta} \int_0^{1-\tilde{\pi}} v^{k^{1+\delta}-1} dv \\
&= \left(1 - \frac{t\delta \log k}{6k^{1+\delta}} \right)^{k^{1+\delta}} \\
&= \left(1 - \frac{t\delta \log k}{6k^{1+\delta}} \right)^{\frac{k^{1+\delta}}{\log k} \log k} \\
&\leq e^{-t(\delta/6) \log k},
\end{aligned}$$

where we used the fact that $(1 - b/x)^x \leq e^{-b}$ for $b \in \mathbb{R}$ and $x > 0$ in the last line. \square

Lemma S4. Suppose that the conditions of Theorem 1 hold. Then $\Pr(\mathcal{A}_n^C) = o(1)$ where the event \mathcal{A}_n is

$$\mathcal{A}_n = \left\{ A_{ii'} (1 \leq i < i' \leq n), Y_{ij} (1 \leq i \leq n, 1 \leq j \leq q) : D_n \geq e^{-C_1 n(n+q)\epsilon_n^2} \right\},$$

for

$$\epsilon_n = \sqrt{\frac{\delta_n k_0 \log k}{n(n+q)}},$$

for some constant $C_1 > 1$.

proof of lemma S4. Denote the KL-neighborhood for the model parameters by

$$\begin{aligned}
\mathcal{B}_n = \left\{ (\boldsymbol{\alpha}, \boldsymbol{\gamma}, \mathbf{Z}, \mathbf{B}) : \frac{2}{n(n+2q-1)} \left(\sum_{i < i'} K(p_{ii'}^A, p_{0ii'}^A) + \sum_{i,j} K(p_{ij}^Y, p_{0ij}^Y) \right) \leq \epsilon_n^2, \right. \\
\left. \frac{2}{n(n+2q-1)} \left(\sum_{i < i'} V(p_{ii'}^A, p_{0ii'}^A) + \sum_{i,j} V(p_{ij}^Y, p_{0ij}^Y) \right) \leq \epsilon_n^2 \right\}.
\end{aligned}$$

For two densities p and q , we let $K(p, q) = \mathbb{E}_p \{\log(p/q)\}$ and $V(p, q) = \mathbb{E}_p \{\log(p/q) - K(p, q)\}^2$ denote the Kullback-Leibler (KL) divergence and second moment of the KL ball, respectively.

By Lemma 10 of Ghosal and van der Vaart (2007), we have for any $C > 0$,

$$\Pr \left\{ D_n \geq e^{-(1+C)n(n+q)\epsilon_n^2} \Pr(\mathcal{B}_n) \right\} \geq 1 - \frac{1}{C^2 n(n+q)\epsilon_n^2},$$

Therefore, it suffices to show that the prior probability $\Pr(\mathcal{B}_n) \geq e^{-C_2 n(n+q)\epsilon_n^2}$ for some $C_2 > 0$. By Taylor expanding $K(p_{ii'}^A, p_{0ii'}^A)$, $K(p_{ij}^Y, p_{0ij}^Y)$, $V(p_{ii'}^A, p_{0ii'}^A)$, and $V(p_{ij}^Y, p_{0ij}^Y)$. Lemma 1 of Jeong and Ghosal (2020) established that

$$\begin{aligned} \max \{K(p_{ii'}^A, p_{0ii'}^A), V(p_{ii'}^A, p_{0ii'}^A)\} &= f_A''(\Theta_{0ii'}^A)(\Theta_{ii'}^A - \Theta_{0ii'}^A)^2 + o\{(\Theta_{ii'}^A - \Theta_{0ii'}^A)^2\}, \\ \max \{V(p_{ij}^Y, p_{0ij}^Y), V(p_{ij}^Y, p_{0ij}^A)\} &= \frac{f_Y''(\Theta_{0ij}^Y)}{\phi}(\Theta_{ij}^Y - \Theta_{0ij}^Y)^2 + o\{(\Theta_{ij}^Y - \Theta_{0ij}^Y)^2\}, \end{aligned}$$

where $f_A(x) = \log(1 + \exp(x))$.

$f_A''(\Theta_{0ii'}^A)$ is bounded by Assumptions S2. And $f_Y''(\Theta_{0ij}^Y) \leq C_f$ by Assumptions S2 and S3. Therefore, $K(p_{ii'}^A, p_{0ii'}^A)$ and $V(p_{ii'}^A, p_{0ii'}^A)$ can be bounded above by a constant multiple of $(\Theta_{ii'}^A - \Theta_{0ii'}^A)^2$ for sufficiently large n . Thus, we have for some constant $b_1 > 0$ which depends on C'_Z , C'_B , C_α , C_γ and C_f/ϕ , and sufficiently large n ,

$$\begin{aligned} \Pr(\mathcal{B}_n) &\geq \Pr \left(\sum_{i < i'} (\Theta_{ii'}^A - \Theta_{0ii'}^A)^2 + \sum_{i,j} (\Theta_{ij}^Y - \Theta_{0ij}^Y)^2 \leq b_1 n(n+q)\epsilon_n^2 \right) \\ &\geq \Pr \left(\sum_{i,i'} (\Theta_{ii'}^A - \Theta_{0ii'}^A)^2 + \sum_{i,j} (\Theta_{ij}^Y - \Theta_{0ij}^Y)^2 \leq b_1 n(n+q)\epsilon_n^2 \right) \\ &= \Pr \left(\|\boldsymbol{\alpha} \mathbf{1}_n^\top + \mathbf{1}_n \boldsymbol{\alpha}^\top + \mathbf{Z} \mathbf{Z}^\top - \boldsymbol{\alpha}_0 \mathbf{1}_n^\top - \mathbf{1}_n \boldsymbol{\alpha}_0^\top - \mathbf{Z}_0 \mathbf{Z}_0^\top\|_F^2 + \|\mathbf{1}_n \boldsymbol{\gamma}^\top + \mathbf{Z} \mathbf{B}^\top - \mathbf{1}_n \boldsymbol{\gamma}_0^\top - \mathbf{Z}_0 \mathbf{B}_0^\top\|_F^2 \leq b_1 n(n+q)\epsilon_n^2 \right) \\ &\geq \Pr \left(\|\boldsymbol{\alpha} \mathbf{1}_n^\top + \mathbf{1}_n \boldsymbol{\alpha}^\top + \mathbf{Z} \mathbf{Z}^\top - \boldsymbol{\alpha}_0 \mathbf{1}_n^\top - \mathbf{1}_n \boldsymbol{\alpha}_0^\top - \mathbf{Z}_0 \mathbf{Z}_0^\top\|_F + \|\mathbf{1}_n \boldsymbol{\gamma}^\top + \mathbf{Z} \mathbf{B}^\top - \mathbf{1}_n \boldsymbol{\gamma}_0^\top - \mathbf{Z}_0 \mathbf{B}_0^\top\|_F \leq \sqrt{b_1 n(n+q)}\epsilon_n \right) \\ &\geq \Pr \left(\|\boldsymbol{\alpha} \mathbf{1}_n^\top + \mathbf{1}_n \boldsymbol{\alpha}^\top - \boldsymbol{\alpha}_0 \mathbf{1}_n^\top - \mathbf{1}_n \boldsymbol{\alpha}_0^\top\|_F \leq \sqrt{\frac{b_1 n(n+q)}{16}}\epsilon_n \right) \times \Pr \left(\|\mathbf{1}_n \boldsymbol{\gamma}^\top - \mathbf{1}_n \boldsymbol{\gamma}_0^\top\|_F \leq \sqrt{\frac{b_1 n(n+q)}{16}}\epsilon_n \right) \times \\ &\quad \Pr \left(\|\mathbf{Z} \mathbf{Z}^\top - \mathbf{Z}_0 \mathbf{Z}_0^\top\|_F + \|\mathbf{Z} \mathbf{B}^\top - \mathbf{Z}_0 \mathbf{B}_0^\top\|_F \leq \sqrt{\frac{b_1 n(n+q)}{4}}\epsilon_n \right), \end{aligned} \tag{S7}$$

where the last line follows from the triangle inequality and the fact that $\boldsymbol{\alpha}$, $\boldsymbol{\gamma}$, \mathbf{Z} and \mathbf{B} is independent of the remaining variables under our prior specification.

Let $\tilde{\mathbf{Z}}_0 = [\mathbf{Z}_0, \mathbf{0}_{n,k-k_0}] \in \mathbb{R}^{n \times k}$ and $\tilde{\mathbf{B}}_0 = [\mathbf{B}_0, \mathbf{0}_{q,k-k_0}] \in \mathbb{R}^{q \times k}$ where $\mathbf{0}_{n,k-k_0}$ and $\mathbf{0}_{q,k-k_0}$ are $n \times (k - k_0)$ and $q \times (k - k_0)$ matrix of zero. Then, we have

$$\begin{aligned} \|\mathbf{Z} \mathbf{Z}^\top - \mathbf{Z}_0 \mathbf{Z}_0^\top\|_F &\leq \|\mathbf{Z} - \tilde{\mathbf{Z}}_0\|_F^2 + 2\|\mathbf{Z}_0\|_2 \|\mathbf{Z} - \tilde{\mathbf{Z}}_0\|, \\ \|\mathbf{Z} \mathbf{B}^\top - \mathbf{Z}_0 \mathbf{B}_0^\top\|_F &\leq \|\mathbf{Z} - \tilde{\mathbf{Z}}_0\|_F \|\mathbf{B} - \tilde{\mathbf{B}}_0\|_F + \|\mathbf{Z}_0\|_2 \|\mathbf{B} - \tilde{\mathbf{B}}_0\|_F + \|\mathbf{B}_0\|_2 \|\mathbf{Z} - \tilde{\mathbf{Z}}_0\|_F. \end{aligned}$$

Combining this with the previous inequality and using Assumptions S2. There exists a constant $b_2 > 0$

such that $2\|\mathbf{Z}_0\|_2 + \|\mathbf{B}_0\|_2 \leq b_2\sqrt{nk_0}$ for sufficiently large n . Let \mathbf{Z}_h and \mathbf{B}_h denote the matrix containing the first h columns of \mathbf{Z} and \mathbf{B} . Then, We have

$$\begin{aligned}
& \Pr \left(\|\mathbf{Z}\mathbf{Z}^\top - \mathbf{Z}_0\mathbf{Z}_0^\top\|_F + \|\mathbf{Z}\mathbf{B}^\top - \mathbf{Z}_0\mathbf{B}_0^\top\|_F \leq \sqrt{\frac{b_1 n(n+q)}{4}} \epsilon_n \right) \\
& \geq \Pr \left(\|\mathbf{Z} - \tilde{\mathbf{Z}}_0\|_F + \|\mathbf{B} - \tilde{\mathbf{B}}_0\|_F \leq \sqrt{\frac{b_1(n+q)}{16b_2k_0}} \epsilon_n \right) \\
& = \mathbb{E} \left\{ \Pr \left(\|\mathbf{Z} - \tilde{\mathbf{Z}}_0\|_F + \|\mathbf{B} - \tilde{\mathbf{B}}_0\|_F \leq \sqrt{\frac{b_1(n+q)}{16b_2k_0}} \epsilon_n \mid \{\pi_h\}_{h=1}^k \right) \right\} \\
& \geq \mathbb{E} \left\{ \Pr \left(\|\mathbf{Z}_{k_0} - \mathbf{Z}_0\|_F \leq \sqrt{\frac{b_1(n+q)}{64b_2k_0}} \epsilon_n \right) \Pr \left(\|\mathbf{B}_{k_0} - \mathbf{B}_0\|_F \leq \sqrt{\frac{b_1(n+q)}{64b_2k_0}} \epsilon_n \right) \prod_{h=1}^{k_0} (1 - \pi_h) \prod_{h=k_0+1}^k \pi_h \right\} \\
& \geq \mathbb{E} \left\{ \prod_{i=1}^n \prod_{h=1}^{k_0} \Pr \left(|z_{ih} - z_{0ih}| \leq \sqrt{\frac{b_1(n+q)}{64b_2k_0^2n}} \epsilon_n \right) \prod_{j=1}^q \prod_{h=1}^{k_0} \Pr \left(|\beta_{jh} - \beta_{0jh}| \leq \sqrt{\frac{b_1(n+q)}{64b_2k_0^2q}} \epsilon_n \right) (1 - \pi_{k_0})^{k_0} \pi_1^{k-k_0} \right\}.
\end{aligned}$$

We have that $\sqrt{b_1(n+q)/64k_0^2n} > b_3/k_0$. some constant $b_3 > 0$ and n sufficiently large. Thus,

$$\begin{aligned}
& \Pr \left(|z_{ih} - z_{0ih}| \leq \sqrt{\frac{b_1(n+q)}{64b_2k_0^2n}} \epsilon_n \right) \geq \Pr \left(|z_{ij} - z_{0ih}| \leq \frac{b_3 \epsilon_n}{k_0} \right) \\
& = \frac{a_\theta \Gamma((2a_\theta - 1)/2)}{b_\theta \Gamma(a_\theta) \sqrt{2\pi a_\theta}} \int_{|z_{ij} - z_{0ih}| \leq b_3 \epsilon_n / k_0} \left(1 + \frac{1}{2a_\theta} \left(\frac{a_\theta z_{ih}}{b_\theta} \right)^2 \right)^{(2a_\theta+1)/2} dz_{ih} \\
& \geq \frac{a_\theta \Gamma((2a_\theta - 1)/2)}{b_\theta \Gamma(a_\theta) \sqrt{2\pi a_\theta}} \left(1 + \frac{1}{2a_\theta} \left(\frac{3a_\theta C_Z}{2b_\theta} \right)^2 \right)^{(2a_\theta+1)/2} \int_{|z_{ij} - z_{0ih}| \leq b_3 \epsilon_n / k_0} dz_{ih} \\
& \geq \frac{b_4 \epsilon_n}{k_0},
\end{aligned}$$

for some constant $b_4 > 0$. Similarly, we have $\sqrt{b_1(n+q)/64k_0^2q} > b_5/k_0$ for some constant $b_5 > 0$ and n sufficiently large. Thus,

$$\begin{aligned}
& \Pr \left(|\beta_{jh} - \beta_{0jh}| \leq \sqrt{\frac{b_1(n+q)}{64b_2k_0^2q}} \epsilon_n \right) \geq \Pr \left(|\beta_{jh} - \beta_{0jh}| \leq \frac{b_5 \epsilon_n}{k_0} \right) \\
& = (2\pi\sigma_B)^{-1/2} \int_{|\beta_{jh} - \beta_{0jh}| \leq b_5 \epsilon_n / k_0} \exp \left(\frac{-\beta_{jh}^2}{2\sigma_B^2} \right) d\beta_{jh} \\
& \geq (2\pi\sigma_B)^{-1/2} \exp \left(\frac{-9C_B^2}{8\sigma_B^2} \right) \int_{|\beta_{jh} - \beta_{0jh}| \leq b_5 \epsilon_n / k_0} d\beta_{jh} \\
& \geq \frac{b_6 \epsilon_n}{k_0},
\end{aligned}$$

for some constant $b_6 > 0$. Furthermore, by jensen inequality we have

$$\mathbb{E} \{ \pi_1^{k-k_0} (1 - \pi_{k_0})^{k_0} \} \geq \left\{ \mathbb{E} \pi_1^{(k-k_0)/k_0 0} (1 - \pi_{k_0}) \right\}^{k_0}.$$

Then for some constant $b_7 > 0$ and n sufficiently large, we have

$$\begin{aligned}
\mathbb{E} \left\{ \pi_1^{(k-k_0)/k_0} (1 - \pi_{k_0}) \right\} &= \mathbb{E} \left\{ v_1^{(k-k_0)/k_0} \left(1 - \sum_{h=1}^{k_0} v_h \prod_{l=1}^{h-1} (1 - v_l) \right) \right\} \\
&= \mathbb{E} \left\{ v_1^{(k-k_0)/k_0} (1 - v_1) \left[1 - v_2 - v_3(1 - v_2) - \dots - v_{k_0} \prod_{l=2}^{k_0-1} (1 - v_l) \right] \right\} \\
&= \frac{k^{1+\delta_n}}{(k^{1+\delta_n} + (k - k_0)/k_0 + 1)(k^{1+\delta_n} + (k - k_0)/k_0)} \left(\frac{1}{a+1} \right)^{k_0-1} \\
&\geq \frac{b_7}{k^{1+\delta_n}} \left(\frac{1}{a+1} \right)^{k_0-1}.
\end{aligned}$$

Hence, for sufficiently large n we have

$$\begin{aligned}
&\Pr \left(\|\mathbf{Z}\mathbf{Z}^\top - \mathbf{Z}_0\mathbf{Z}_0^\top\|_F + \|\mathbf{Z}\mathbf{B}^\top - \mathbf{Z}_0\mathbf{B}_0^\top\|_F \leq \sqrt{\frac{b_1 n(n+q)}{4}} \epsilon_n \right) \\
&\geq \exp \left(-\frac{1}{2} (nk_0 + qk_0) \log(k_0 n(n+q) - \delta_n \log k - 2(b_4 + b_6)) - (1 + \delta_n)k_0 \log k - k_0(k_0 - 1) \log(a+1) \right) \\
&\geq \exp \left(-\tilde{C} \delta_n k_0 \log n - (1 + \delta_n)k_0 \log k \right) \geq \exp \left(-(\tilde{C}/\lambda) \delta_n k_0 \log k - (1 + \delta_n)k_0 \log k \right) \\
&\geq \exp(-C_3 \delta_n k_0 \log k) \\
&\geq \exp(-C_3 n(n+q) \epsilon_n^2).
\end{aligned}$$

for some universal constant \tilde{C} and $C_3 = \tilde{C}/\lambda + 2$. Then

$$\begin{aligned}
&\Pr \left(\|\boldsymbol{\alpha} \mathbf{1}_n^\top + \mathbf{1}_n \boldsymbol{\alpha}^\top - \boldsymbol{\alpha}_0 \mathbf{1}_n^\top + \mathbf{1}_n \boldsymbol{\alpha}_0^\top\|_F \leq \sqrt{\frac{b_1 n(n+q)}{16}} \epsilon_n \right) \\
&\geq \Pr \left(\|(\boldsymbol{\alpha} - \boldsymbol{\alpha}_0)\|_2 \leq \sqrt{\frac{b_1(n+q)}{64}} \epsilon_n \right) \\
&\geq \prod_{i=1}^n \Pr \left(|\alpha_i - \alpha_{0i}| \leq \sqrt{\frac{b_1(n+q)}{64n}} \epsilon_n \right) \\
&\geq (b_8 \epsilon_n)^n = \exp(-(n/2) \log n(n+q) + (n/2) \log(\delta_n k_0 \log k + 2b_8)) \\
&\geq \exp(-b_9 \delta_n \log n) \geq \exp(-(b_9/\lambda) \delta_n \log k) \\
&\geq \exp(-C_4 n(n+q) \epsilon_n^2).
\end{aligned}$$

Similarly, we have

$$\begin{aligned}
&\Pr \left(\|\mathbf{1}_n \boldsymbol{\gamma}^n - \mathbf{1}_n \boldsymbol{\gamma}_0^n\|_F \leq \sqrt{\frac{b_1 n(n+q)}{16}} \epsilon_n \right) \\
&\geq \prod_{j=1}^q \Pr \left(|\gamma_j - \gamma_{0j}| \leq \sqrt{\frac{b_1(n+q)}{16q}} \epsilon_n \right) \\
&\geq (b_{10} \epsilon_n)^q = \exp(-q/2 \log n(n+q) + q/2 \log(\delta_n k_0 \log k + 2b_{10})) \\
&\geq \exp(-b_{11} \delta_n \log n) \geq \exp(-(b_{11}/\lambda) \delta_n \log k) \\
&\geq \exp(-C_5 n(n+q) \epsilon_n^2).
\end{aligned}$$

Combining the previous three bounds for the probabilities in Eq. (S7) with $C_1 = \max(C_3, C_4, C_5)$ gives the desired bound on $\Pr(\mathcal{B}_n)$. The result follows $C_1 = 1 + C + C_2$. \square

B.3.2 Proof of Theorem 1 (Posterior Concentration for the Latent Dimension)

Proof of Theorem 1. We prove this result for a general fractional posterior. We write the fractional posterior probability as

$$\Pr(K^* > Ck_0 \mid \mathbf{A}, \mathbf{Y}) = \frac{N_n(\{\mathbf{Z} : K^* > Ck_0\})}{D_n}, \quad (\text{S8})$$

where $N_n(\cdot)$ and D_n are defined in Eq. (S5) and (S6). Now, we introduce an event \mathcal{A}_n with large probability under the true data generating process. In particular, $\mathcal{A}_n = \{\mathbf{A}, \mathbf{Y} : D_n \geq e^{-C_1 n(n+q)\epsilon_n^2}\}$, where ϵ_n is the rate in Lemma S4. If we decompose the probability in Eq. (S8) into the sum of two complementary conditional probabilities (conditioning on \mathcal{A}_n and \mathcal{A}_n^C), we can write:

$$\mathbb{E}_0 \{\Pr(K^* > Ck_0 \mid \mathbf{A}, \mathbf{Y})\} \leq \mathbb{E}_0 \{\Pr(K^* > Ck_0 \mid \mathbf{A}, \mathbf{Y}) \mathbb{1}(\mathcal{A}_n)\} + \Pr(\mathcal{A}_n^C).$$

On the event \mathcal{A}_n , D_n is bounded below by $e^{-C_1 \delta_n k_0 \log k}$. On the other hand, the expected value of the numerator can be bounded above by $\Pr(K^* > Ck_0)$ using Fubini's theorem

$$\begin{aligned} & \mathbb{E}_0 \left\{ \int \int \int_{K^* > Ck_0} \prod_{i < i'} \frac{p_{\Theta_{ii'}^A}(A_{ii'})}{p_{\Theta_{0ii'}^A}(A_{ii'})} \prod_{i,j} \frac{p_{\Theta_{ij}^Y}(Y_{ij})}{p_{\Theta_{0ij}^Y}(Y_{ij})} d\Pi(\boldsymbol{\alpha}) d\Pi(\boldsymbol{\gamma}) d\Pi(\mathbf{Z}) d\Pi(\mathbf{B}) \right\} \\ &= \int \int \int_{K^* > Ck_0} \prod_{i < i'} \prod_{i,j} \mathbb{E}_0 \left\{ \frac{p_{\Theta_{ii'}^A}(A_{ii'})}{p_{\Theta_{0ii'}^A}(A_{ii'})} \frac{p_{\Theta_{ij}^Y}(Y_{ij})}{p_{\Theta_{0ij}^Y}(Y_{ij})} \right\} d\Pi(\boldsymbol{\alpha}) d\Pi(\boldsymbol{\gamma}) d\Pi(\mathbf{Z}) d\Pi(\mathbf{B}) \leq \Pr(K^* > Ck_0) \end{aligned}$$

Therefore, we can use Lemma S4 to conclude that

$$\mathbb{E}_0 \{\Pr(K^* > Ck_0 \mid \mathbf{A}, \mathbf{Y})\} \leq \Pr(K^* > Ck_0) e^{C_1 \delta_n k_0 \log k} + o(1),$$

In addition, for n sufficiently large we have that $\delta_n > 6/\log k$, since $k = \lceil n^\lambda \rceil$ by Assumption S1, so we can apply Lemma S3 to bound the previous expression from above as

$$\mathbb{E}_0 \{\Pr(K^* > Ck_0 \mid A, Y)\} \leq 3e^{-(C/6 - C_1)\delta_n k_0 \log k} + o(1),$$

for n large enough, which goes to zero as $n \rightarrow \infty$ and $C > \max\{6C_1, 1\}$. Lastly, C_1 increases with the constants C_3, C_4 and C_5 defined in the proof of Lemma S4 which depend on the type of node variable and increase with λ^{-1} . \square

B.3.3 Proof of Theorem 2 (Posterior Contraction Rate)

Proof of theorem 2. Define the contraction rate $\epsilon_n = (k_0 \log k/n)^{1/2}$ and the event $\mathcal{E}_n = \{(\boldsymbol{\alpha}, \boldsymbol{\gamma}, \mathbf{Z}, \mathbf{B}) : K^* \leq C_1 k_0\}$ for C_1 in Theorem 1. For a large enough constant $C_2 > 0$, we have that

$$\begin{aligned} & \mathbb{E}_0 [\Pr \{(\boldsymbol{\alpha}, \boldsymbol{\gamma}, \mathbf{Z}, \mathbf{B}) : H_n(\boldsymbol{\Theta}, \boldsymbol{\Theta}_0) > C_2 \epsilon_n \mid \mathbf{A}, \mathbf{Y}\}] \\ & \leq \mathbb{E}_0 [\Pr \{(\boldsymbol{\alpha}, \boldsymbol{\gamma}, \mathbf{Z}, \mathbf{B}) \in \mathcal{E}_n : H_n(\boldsymbol{\Theta}, \boldsymbol{\Theta}_0) > C_2 \epsilon_n \mid \mathbf{A}, \mathbf{Y}\} \mathbb{1}(\mathcal{A}_n)] + \mathbb{E}_0 \{\Pr(\mathcal{E}_n^C \mid \mathbf{A}, \mathbf{Y})\} + \Pr(\mathcal{A}_n^C), \end{aligned}$$

where $\mathcal{A}_n = \{\mathbf{A}, \mathbf{Y} : D_n \geq e^{-C_1 \delta_n k_0 \log k}\}$ is the event in Lemma S4. Also, on the event \mathcal{A}_n the denominator $D_n \geq e^{-C'_1 n k_0 \log k} > e^{-C'_1 n(n+q)\epsilon^2}$ for some constant C'_1 . By Theorem 1 and Lemma S4, the last two terms tend to zero as $n \rightarrow \infty$. It remains to show that the first term also goes to zero. To do so, we use the prior-mass-and-testing technique introduced in Ghosal et al. (2000), which involves constructing an appropriate sieve $\mathcal{F}_n \subset \mathcal{E}_n$ and a uniformly consistent sequence of test functions Φ_n such that for all $\epsilon > \epsilon_n$,

$$\begin{aligned} \Pr(\mathcal{E}_n \setminus \mathcal{F}_n) & \lesssim \exp\{-(1 + C'_1)n(n+1)\epsilon_n^2\}, \\ \mathbb{E}_0(\Phi_n) & \lesssim \exp(-Cn(n+1)\epsilon_n^2), \\ \sup_{(\boldsymbol{\alpha}, \boldsymbol{\gamma}, \mathbf{Z}, \mathbf{B}) \in \mathcal{F}_n : H_n(\boldsymbol{\Theta}, \boldsymbol{\Theta}_0) > \epsilon} \mathbb{E}_\Theta(1 - \Phi_n) & \lesssim \exp(-Cn(n+1)\epsilon_n^2), \end{aligned} \tag{S9}$$

where \mathbb{E}_Θ denotes the expectation under the model with parameters $(\boldsymbol{\alpha}, \boldsymbol{\gamma}, \mathbf{Z}, \mathbf{B})$ and $\boldsymbol{\Theta} = [\boldsymbol{\alpha} \mathbf{1}_n^\top + \mathbf{1}_n \boldsymbol{\alpha}^\top + \mathbf{Z} \mathbf{Z}^\top, \mathbf{1}_n \boldsymbol{\gamma}^\top + \mathbf{Z} \mathbf{B}^\top]$ and the constant $C > C'_1$.

Before constructing such a sieve and test functions Φ_n , we demonstrate that their existence implies the Hellinger consistency of the posterior distribution. We use a standard argument originally Schwartz (1965). Since Φ_n and the posterior probability are less than or equal to one, we have that

$$\begin{aligned} & \mathbb{E}_0 [\Pr \{(\boldsymbol{\alpha}, \boldsymbol{\gamma}, \mathbf{Z}, \mathbf{B}) \in \mathcal{E}_n : H_n(\boldsymbol{\Theta}, \boldsymbol{\Theta}_0) > C_2 \epsilon_n \mid \mathbf{A}, \mathbf{Y}\} \mathbb{1}(\mathcal{A}_n)] \\ & \leq \mathbb{E}_0 [\Pr \{(\boldsymbol{\alpha}, \boldsymbol{\gamma}, \mathbf{Z}, \mathbf{B}) \in \mathcal{E}_n : H_n(\boldsymbol{\Theta}, \boldsymbol{\Theta}_0) > C_2 \epsilon_n \mid \mathbf{A}, \mathbf{Y}\} \mathbb{1}(\mathcal{A}_n)(1 - \Phi_n)] + \mathbb{E}_0(\Phi_n) \\ & \leq \left\{ \sup_{(\boldsymbol{\alpha}, \boldsymbol{\gamma}, \mathbf{Z}, \mathbf{B}) \in \mathcal{F}_n : H_n(\boldsymbol{\Theta}, \boldsymbol{\Theta}_0) > C_2 \epsilon_n} \mathbb{E}_\Theta(1 - \Phi_n) + \Pr(\mathcal{E}_n \setminus \mathcal{F}_n) \right\} e^{C'_1 n(n+q)\epsilon^2} + \mathbb{E}_0(\Phi_n), \end{aligned} \tag{S10}$$

where the last inequality follows from an application of Fubini's theorem and the definition of the event \mathcal{A}_n . We have that $\Pr(\mathcal{E}_n \setminus \mathcal{F}_n) e^{C'_1 n(n+1)\epsilon_n^2} \lesssim e^{-n(n+1)\epsilon_n^2}$, which goes to zero as $n \rightarrow \infty$. Since $C > C'_1$, the remaining two terms go to zero as long as $C_2 > 1$. To complete the proof, we proceed to construct the appropriate sieve and test functions satisfying (S10).

Sieve construction. First, we introduce some notation. For matrix $\mathbf{Z} \in \mathbb{R}^{n \times k}$ and $\mathbf{B} \in \mathbb{R}^{q \times k}$, and a set $S \subset \{1, \dots, k\}$, we use the notation $\mathbf{Z}_S = (\mathbf{Z}_j)_{j \in S} \in \mathbb{R}^{n \times |S|}$ and $\mathbf{B}_S = (\mathbf{B}_j)_{j \in S} \in \mathbb{R}^{q \times |S|}$, that the matrix constructed from \mathbf{Z} and \mathbf{B} by including only columns in S . Define the the sieve

$$\begin{aligned} \mathcal{F}_n = \{(\boldsymbol{\alpha}, \boldsymbol{\gamma}, \mathbf{Z}, \mathbf{B}) \in \mathbb{R}^n \times \mathbb{R}^q \times \mathbb{R}^{n \times k} \times \mathbb{R}^{q \times k} : \\ \|\boldsymbol{\alpha}\|_2 \leq L_n, \|\boldsymbol{\gamma}\|_2 \leq L_n, \|\mathbf{Z}\|_F \leq L_n, \|\mathbf{B}\|_F \leq L_n, K^* \leq C_1 k_0\} \subset \mathcal{E}_n. \end{aligned}$$

where $L_n = M_1 n^{M_2}$ and $M_1, M_2 > 0$, are constants chosen subsequently so that the prior probability of falling out side the sieve is bounded above by $e^{-(1+C'_1)n(n+q)\epsilon_n^2}$. Under the prior, we have that

$$\Pr(\mathcal{E}_n \setminus \mathcal{F}_n) \leq \Pr(\|\boldsymbol{\alpha}\|_2 > L_n) + \Pr(\|\boldsymbol{\gamma}\|_2 > L_n) + \Pr(\|\mathbf{Z}\|_F > L_n, K^* \leq C_1 k_0) + \Pr(\|\mathbf{B}\|_F > L_n, K^* \leq C_1 k_0),$$

We bound each probability in turn starting with the second term. We have that

$$\Pr(\|\mathbf{Z}\|_F > L_n, K^* \leq C_1 k_0) = \mathbb{E}\{\Pr(\|\mathbf{Z}\|_F > L_n, K^* \leq C_1 k_0 \mid \{\pi_h\}_{h=1}^k)\},$$

where

$$\begin{aligned} \Pr(\|\mathbf{Z}\|_F > L_n, K^* \leq C_1 k_0 \mid \{\pi_h\}_{h=1}^k) &= \sum_{S: 1 \leq |S| \leq C_1 k_0} \Pr(S \mid \{\pi_h\}_{h=1}^k) \Pr(\|\mathbf{Z}_S\|_F > L_n) \\ &\leq \sum_{S: 1 \leq |S| \leq C_1 k_0} \Pr(\|\mathbf{Z}_S\|_F > L_n), \end{aligned} \tag{S11}$$

Since $\|\mathbf{Z}_S\|_F^2 = \sum_{i=n} \sum_{j \in S} z_{ij}^2$ is a sum of independent and identically distributed random variables with expectation $b_{z1} = b_\theta/(a_\theta - 1)$ and variance $b_{z2} = 3b_\theta^2/((a_\theta - 1)(a_\theta - 2))$. Then for n lager enough

$$\Pr(\|\mathbf{Z}_S\|_F > L_n) = \Pr\left(\frac{\sum_{i=n} \sum_{j \in S} z_{ij}^2 - n|S|b_{z1}}{\sqrt{n|S|b_{z2}}} > \frac{L_n^2 - n|S|b_{z1}}{\sqrt{n|S|b_{z2}}}\right) \leq \exp\left\{-\frac{(L_n^2 - n|S|b_{z1})^2}{2n|S|b_{z2}}\right\},$$

We can choose $M_2 > 1/2$, there exist constant b_1 for n lager enough such that,

$$\Pr(\|\mathbf{Z}_S\|_F > L_n) \leq \exp\{-(b_1/k_0)M_1^4 n^{4M_2-1}\},$$

Plugging the previous expression into Eq. (S11) and noting that the bound is independent of $\{\pi_h\}_{h=1}^k$, we have

$$\begin{aligned} \Pr(\|\mathbf{Z}\|_F > L_n, K^* \leq C_1 k_0) &\leq \sum_{s=1}^{\lfloor C_1 k_0 \rfloor} \binom{k}{s} \exp\{-(b_1/k_0)M_1^4 n^{4M_2-1}\} \\ &\leq \sum_{s=1}^{\lfloor C_1 k_0 \rfloor} \left(\frac{ek}{s}\right)^s \exp\{-(b_1/k_0)M_1^4 n^{4M_2-1}\} \\ &\leq \exp\{-(b_1/k_0)M_1^4 n^{4M_2-1} + C_1 k_0 \log k + \log C_1 k_0 + C_1 k_0\} \\ &\leq \exp\{-(b_1/k_0)M_1^4 n^{4M_2-1} + b_2 n k_0 \log k\}, \end{aligned}$$

for some constant $b_2 > 0$ where we use the inequality $\binom{k}{s} \leq \left(\frac{ek}{s}\right)^s$ in the second line. Due to Assumption S1, we can choose that $M_2 > 1$ so that $n^{4M_2-1}/k_0 > n^2 \log n > n k_0 \log k$. With this choice of M_2 , we have

$$\begin{aligned} \Pr(\|\mathbf{Z}\|_F > L_n, K^* \leq C_1 k_0) &\leq \exp\{-(b_1 M_1^4 - b_2 + 1) n k_0 \log k\} \\ &\leq \exp\{-(1 + C'_1)n(n+q)\epsilon_n^2\}, \end{aligned}$$

when we set $M_1 > ((C'_1 + b_2)/b_1)^{1/4}$.

Similarly, we have that

$$\Pr(\|\mathbf{B}\|_F > L_n, K^* \leq C_1 k_0) \leq \sum_{S: 1 \leq |S| \leq C_1 k_0} \Pr(\|\mathbf{B}_S\|_F > L_n),$$

And we have that $(1/\sigma_B^2)\|\mathbf{B}_S\|_F^2 \sim \Gamma(n|S|/2, 2)$. Similar as the proof of Loyal and Chen (2025), we use the sub-gamma tail bound in Lemma S1 to conclude that

$$\Pr(\|\mathbf{B}_S\|_F > L_n) \leq \exp\{-(1/4\sigma_B^2)M_1^2 n^{2M_2} + nC_1 k_0\},$$

Then we have that

$$\begin{aligned} \Pr(\|\mathbf{B}\|_F > L_n, K^* \leq C_1 k_0) &\leq \sum_{s=1}^{\lfloor C_1 k_0 \rfloor} \binom{k}{s} \exp\{-(1/4\sigma_B^2)M_1^2 n^{2M_2} + nC_1 k_0\} \\ &\leq \sum_{s=1}^{\lfloor C_1 k_0 \rfloor} \left(\frac{ek}{s}\right)^s \exp\{-(1/4\sigma_B^2)M_1^2 n^{2M_2} + nC_1 k_0\} \\ &\leq \exp\{-(1/4\sigma_B^2)M_1^2 n^{2M_2} + b_3 n k_0 \log k\}, \end{aligned}$$

for some constant $b_3 > 0$. We can choose $M_2 > 3/2$ so that $n^{2M_2} > n^2 \log n > n k_0 \log k$. We have

$$\begin{aligned} \Pr(\|\mathbf{B}\|_F > L_n, K^* \leq C_1 k_0) &\leq \exp\{-(1/4\sigma_B^2)M_1^2 n^{2M_2} - b_3 + 1\} n k_0 \log k \\ &\leq \exp\{-(1 + C'_1)n(n+q)\epsilon_n^2\}, \end{aligned}$$

when we set $M_1 > \max\{2\sigma_B\sqrt{C'_1 + b_3}, ((C'_1 + b_2)/b_1)^{1/4}\}$.

Similarly, we have that $(1/\sigma_\alpha^2)\|\boldsymbol{\alpha}\|_2^2 \sim \Gamma(n/2, 2)$ and $(1/\sigma_\gamma^2)\|\boldsymbol{\gamma}\|_2^2 \sim \Gamma(n/2, 2)$. So we use the sub-gamma tail bound in Lemma S1 to conclude that

$$\begin{aligned} \Pr(\|\boldsymbol{\alpha}\|_2^2 > L_n) &\leq \exp\{-(1/4\sigma_\alpha^2)M_1^2 n^{2M_2} + n\} \leq \exp\{-(1 + C'_1)n(n+q)\epsilon_n^2\}, \\ \Pr(\|\boldsymbol{\gamma}\|_2^2 > L_n) &\leq \exp\{-(1/4\sigma_\gamma^2)M_1^2 n^{2M_2} + q\} \leq \exp\{-(1 + C'_1)n(n+q)\epsilon_n^2\}, \end{aligned}$$

due to our previous choice of M_2 and when we set $M_1 > \max\{2\sigma_\alpha\sqrt{C'_1 + 1}, 2\sigma_\gamma\sqrt{C'_1 + 1}, 2\sigma_B\sqrt{C'_1 + b_3}, ((C'_1 + b_2)/b_1)^{1/4}\}$

Test construction. By Lemma 2 of Ghosal and van der Vaart (2007) there exist local test functions ϕ_n , such that for any $\boldsymbol{\alpha}, \boldsymbol{\gamma}, \mathbf{Z}, \mathbf{B}$ with $H_n(\boldsymbol{\Theta}_1, \boldsymbol{\Theta}_0) > \epsilon$,

$$\mathbb{E}_0(\phi_n) \leq \exp(-n(n+q)\epsilon^2/4), \quad \sup_{(\boldsymbol{\alpha}, \boldsymbol{\gamma}, \mathbf{Z}, \mathbf{B}) \in \mathcal{F}_n: H_n(\boldsymbol{\Theta}_1, \boldsymbol{\Theta}_0) > \epsilon/18} \mathbb{E}_\Theta(1 - \phi_n) \lesssim \exp(-n(n+q)\epsilon_n^2/4).$$

To construct a uniformly consistent test over the sieve, we aim to apply Lemma 9 of Ghosal and van der Vaart (2007), which constructs this test by combining these local tests using an ϵ -net argument. As such, we need to control the metric entropy of the sieve. In particular, we must show that

$\log N(\epsilon_n/36, \mathcal{F}_n, H_n) \lesssim n(n+q)\epsilon_n^2$. To do so we re-express $\mathcal{F}_n = \cup_{S:|S| \leq C_1 k_0} \mathcal{F}_n(S)$ where

$$\begin{aligned} \mathcal{F}_n = \{(\boldsymbol{\alpha}, \boldsymbol{\gamma}, \mathbf{Z}, \mathbf{B}) \in \mathbb{R}^n \times \mathbb{R}^q \times \mathbb{R}^{n \times k} \times \mathbb{R}^{q \times k} : \\ \|\boldsymbol{\alpha}\|_2 \leq L_n, \|\boldsymbol{\gamma}\|_2 \leq L_n, \|\mathbf{Z}_S\|_F \leq L_n, \|\mathbf{B}_S\|_F \leq L_n, \mathbf{Z}_{S^C} = \mathbf{0}\}. \end{aligned}$$

Since a union bound implies $N(\epsilon_n/36, \mathcal{F}_n, H_n) \leq \sum_{S:|S| \leq C_1 k_0} N(\epsilon_n/36, \mathcal{F}_n(S), H_n)$, we start by upper bounding $N(\epsilon_n/36, \mathcal{F}_n(S), H_n)$ for given S .

First, we relate the metric entropy under H_n to more natural metrics on the parameter space using an argument developed in Jeong and Ghosal (2020). Since the squared Hellinger distance is bounded by the KL divergence, we have for any $(\boldsymbol{\alpha}_1, \boldsymbol{\gamma}_1, \mathbf{Z}_1, \mathbf{B}_1), (\boldsymbol{\alpha}_2, \boldsymbol{\gamma}_2, \mathbf{Z}_2, \mathbf{B}_2) \in \mathcal{F}_n$ with $\boldsymbol{\Theta}_1^A = \boldsymbol{\alpha}_1 \mathbf{1}_n^\top + \mathbf{1}_n \boldsymbol{\alpha}_1^\top + \mathbf{Z}_1 \mathbf{Z}_1^\top$, $\boldsymbol{\Theta}_1^Y = \mathbf{1}_n \boldsymbol{\gamma}_1^\top + \mathbf{Z}_1 \mathbf{B}_1^\top$, $\boldsymbol{\Theta}_2^A = \boldsymbol{\alpha}_2 \mathbf{1}_n^\top + \mathbf{1}_n \boldsymbol{\alpha}_2^\top + \mathbf{Z}_2 \mathbf{Z}_2^\top$ and $\boldsymbol{\Theta}_2^Y = \mathbf{1}_n \boldsymbol{\gamma}_2^\top + \mathbf{Z}_2 \mathbf{B}_2^\top$ that

$$\begin{aligned} h^2(p_{1ii'}^A, p_{2ii'}^A) &\leq K(p_{1ii'}^A, p_{2ii'}^A) = f_A''(\boldsymbol{\Theta}_{1ii'}^A)(\boldsymbol{\Theta}_{1ii'}^A - \boldsymbol{\Theta}_{2ii'}^A)^2 + o\{(\boldsymbol{\Theta}_{1ii'}^A - \boldsymbol{\Theta}_{2ii'}^A)^2\}, \\ h^2(p_{1ij}^Y, p_{2ij}^A) &\leq K(p_{1ij}^Y, p_{2ij}^A) = \frac{f_Y''(\boldsymbol{\Theta}_{1ij}^Y)}{\phi}(\boldsymbol{\Theta}_{1ij}^Y - \boldsymbol{\Theta}_{2ij}^A)^2 + o\{(\boldsymbol{\Theta}_{1ij}^Y - \boldsymbol{\Theta}_{2ij}^A)^2\}, \end{aligned}$$

by a Taylor expansion. Next for any $(\boldsymbol{\alpha}_1, \boldsymbol{\gamma}_1, \mathbf{Z}_1, \mathbf{B}_1) \in \mathcal{F}_n(S)$ for a given S , we have that $|\boldsymbol{\Theta}_{1ii'}^A| \leq L_n(2 + L_n)$ and $|\boldsymbol{\Theta}_{1ij}^Y| \leq L_n(1 + L_n)$. Let $\psi_A(L_n) = 1 + \sup_{x:x \leq L_n(2+L_n)} f_A''(x)$ where $f_A(x) = \log(1 + \exp(x))$. Recall $\psi_Y(L_n) = 1 + \sup_{x:x \leq L_n(1+L_n)} f_Y''(x)$, so that

$$\begin{aligned} h^2(p_{1ii'}^A, p_{2ii'}^A) &\leq \psi_A(L_n)(\boldsymbol{\Theta}_{1ii'}^A - \boldsymbol{\Theta}_{2ii'}^A)^2 + o\{(\boldsymbol{\Theta}_{1ii'}^A - \boldsymbol{\Theta}_{2ii'}^A)^2\}, \\ h^2(p_{1ij}^Y, p_{2ij}^A) &\lesssim \psi_Y(L_n)(\boldsymbol{\Theta}_{1ij}^Y - \boldsymbol{\Theta}_{2ij}^A)^2 + o\{(\boldsymbol{\Theta}_{1ij}^Y - \boldsymbol{\Theta}_{2ij}^A)^2\}, \end{aligned}$$

for any $(\boldsymbol{\alpha}_1, \boldsymbol{\gamma}_1, \mathbf{Z}_1, \mathbf{B}_1), (\boldsymbol{\alpha}_2, \boldsymbol{\gamma}_2, \mathbf{Z}_2, \mathbf{B}_2) \in \mathcal{F}_n$. If $|\boldsymbol{\Theta}_{1ii'}^A - \boldsymbol{\Theta}_{2ii'}^A| \leq \{\sum_{i < i'} (\boldsymbol{\Theta}_{1ii'}^A - \boldsymbol{\Theta}_{2ii'}^A)^2\}^{1/2} \leq \psi_Y(L_n)^{-1/2} \epsilon_n$ and $|\boldsymbol{\Theta}_{1ij}^Y - \boldsymbol{\Theta}_{2ij}^A| \leq \{\sum_{ij} (\boldsymbol{\Theta}_{1ij}^Y - \boldsymbol{\Theta}_{2ij}^A)^2\}^{-1/2} \leq \psi_Y(L_n)^{-1/2} \epsilon_n$ which tends to zero since $\psi_A(L_n), \psi_Y(L_n) \geq 1$, let $\psi(L_n) = \max\{\psi_A(L_n), \psi_Y(L_n)\}$, the root-averaged-squared Hellinger metric satisfies

$$H_n(p_{\Theta_1}, p_{\Theta_2}) \lesssim \left\{ \frac{2\psi(L_n)}{n(n+q)} \left(\sum_{i < i'} (\boldsymbol{\Theta}_{1ii'}^A - \boldsymbol{\Theta}_{2ii'}^A)^2 + \sum_{ij} (\boldsymbol{\Theta}_{1ij}^Y - \boldsymbol{\Theta}_{2ij}^A)^2 \right) \right\}^{\frac{1}{2}} \leq \epsilon_n,$$

for any $(\boldsymbol{\alpha}_1, \boldsymbol{\gamma}_1, \mathbf{Z}_1, \mathbf{B}_1), (\boldsymbol{\alpha}_2, \boldsymbol{\gamma}_2, \mathbf{Z}_2, \mathbf{B}_2) \in \mathcal{F}_n$. Furthermore,

$$\begin{aligned} &\left\{ \sum_{i < i'} (\boldsymbol{\Theta}_{1ii'}^A - \boldsymbol{\Theta}_{2ii'}^A)^2 + \sum_{ij} (\boldsymbol{\Theta}_{1ij}^Y - \boldsymbol{\Theta}_{2ij}^A)^2 \right\}^{\frac{1}{2}} \\ &\leq \|\boldsymbol{\alpha}_1 \mathbf{1}_n^\top + \mathbf{1}_n \boldsymbol{\alpha}_1^\top + \mathbf{Z}_1 \mathbf{Z}_1^\top - \boldsymbol{\alpha}_2 \mathbf{1}_n^\top - \mathbf{1}_n \boldsymbol{\alpha}_2^\top - \mathbf{Z}_2 \mathbf{Z}_2^\top\|_F + \|\mathbf{1}_n \boldsymbol{\gamma}_1^\top + \mathbf{Z}_1 \mathbf{B}_1^\top - \mathbf{1}_n \boldsymbol{\gamma}_2^\top - \mathbf{Z}_2 \mathbf{B}_2^\top\|_F \\ &\leq 2\sqrt{n} \|\boldsymbol{\alpha}_1 - \boldsymbol{\alpha}_2\|_2 + \sqrt{n} \|\boldsymbol{\gamma}_1 - \boldsymbol{\gamma}_2\|_2 + 7L_n \|\mathbf{Z}_1 - \mathbf{Z}_2\|_F + L_n \|\mathbf{B}_1 - \mathbf{B}_2\|_F, \end{aligned}$$

for any $(\boldsymbol{\alpha}_1, \boldsymbol{\gamma}_1, \mathbf{Z}_1, \mathbf{B}_1), (\boldsymbol{\alpha}_2, \boldsymbol{\gamma}_2, \mathbf{Z}_2, \mathbf{B}_2) \in \mathcal{F}_n$, using the argument presented in the proof of Lemma S4. Based on the above bound, for some constant $b_4 > 0$, the metric entropy $\log N(\epsilon_n/36, \mathcal{F}_n(S), H_n)$ is

bounded above by

$$\begin{aligned} & \log N \left(\frac{b_4 \epsilon_n / 288}{(n\psi(L_n))^{1/2}}, \{\boldsymbol{\alpha} \in \mathbb{R}^n : \|\boldsymbol{\alpha}\|_2 \leq L_n\}, \|\cdot\|_2 \right) + \log N \left(\frac{b_4 \epsilon_n / 144}{(n\psi(L_n))^{1/2}}, \{\boldsymbol{\gamma} \in \mathbb{R}^q : \|\boldsymbol{\gamma}\|_2 \leq L_n\}, \|\cdot\|_2 \right) \\ & + \log N \left(\frac{b_4 \epsilon_n / 1008}{\psi(L_n)^{1/2} L_n}, \{\mathbf{Z} \in \mathbb{R}^{n \times |S|} : \|\mathbf{Z}\|_F \leq L_n\}, \|\cdot\|_F \right) + \log N \left(\frac{b_4 \epsilon_n / 144}{\psi(L_n)^{1/2} L_n}, \{\mathbf{B} \in \mathbb{R}^{q \times |S|} : \|\mathbf{B}\|_F \leq L_n\}, \|\cdot\|_F \right), \end{aligned}$$

We bound each term separately. In what follows, recall that the ϵ -covering number of a d -dimensional Euclidean ball of radius r under the l_2 metric is upper bounded by $(3r/\epsilon)^d$ for $\epsilon \in (0, 1]$. Then we have

$$\begin{aligned} \log N \left(\frac{b_4 \epsilon_n / 288}{(n\psi(L_n))^{1/2}}, \{\boldsymbol{\alpha} \in \mathbb{R}^n : \|\boldsymbol{\alpha}\|_2 \leq L_n\}, \|\cdot\|_2 \right) & \leq \log \left\{ \frac{864(n\psi(L_n))^{1/2} L_n}{b_2 \epsilon_n} \right\}^n \\ & \lesssim n \log n \\ & \lesssim n(n+q)\epsilon_n^2, \end{aligned}$$

and

$$\begin{aligned} \log N \left(\frac{b_4 \epsilon_n / 144}{(n\psi(L_n))^{1/2}}, \{\boldsymbol{\gamma} \in \mathbb{R}^q : \|\boldsymbol{\gamma}\|_2 \leq L_n\}, \|\cdot\|_2 \right) & \leq \log \left\{ \frac{432(n\psi(L_n))^{1/2} L_n}{b_2 \epsilon_n} \right\}^q \\ & \lesssim q \log n \\ & \lesssim n(n+q)\epsilon_n^2, \end{aligned}$$

and

$$\begin{aligned} \log N \left(\frac{b_4 \epsilon_n / 1008}{\psi(L_n)^{1/2} L_n}, \{\mathbf{Z} \in \mathbb{R}^{n \times |S|} : \|\mathbf{Z}\|_F \leq L_n\}, \|\cdot\|_F \right) & \leq \log \left\{ \frac{3024\psi(L_n)^{1/2} L_n^2}{b_2 \epsilon_n} \right\}^{n \times k_0} \\ & \lesssim n k_0 \log n \\ & \lesssim n(n+q)\epsilon_n^2, \end{aligned}$$

and

$$\begin{aligned} \log N \left(\frac{b_4 \epsilon_n / 144}{\psi(L_n)^{1/2} L_n}, \{\mathbf{B} \in \mathbb{R}^{q \times |S|} : \|\mathbf{B}\|_F \leq L_n\}, \|\cdot\|_F \right) & \leq \log \left\{ \frac{432\psi(L_n)^{1/2} L_n^2}{b_2 \epsilon_n} \right\}^{q \times k_0} \\ & \lesssim q k_0 \log n \\ & \lesssim n(n+q)\epsilon_n^2, \end{aligned}$$

where we used Assumption S3 to conclude that $\log \psi(L_n) + \log L_n \lesssim \log n$. Combining these bounds, we find that for some constant $b_5 > 0$, the metric entropy of the sieve $\log N(\epsilon_n/36, \mathcal{F}_n, H_n)$ is bounded by

$$\begin{aligned} \log \left\{ \sum_{S: |S| \leq C_1 k_0} N\left(\frac{\epsilon_n}{36}, \mathcal{F}_n(S), H_n\right) \right\} & \leq \log \left\{ \sum_{s=0}^{\lfloor C_1 k_0 \rfloor} \binom{k}{s} e^{b_5 n(n+q)\epsilon_n^2} \right\} \\ & \lesssim \log(C_1 k_0 + 1) C_1 k_0 \log k + b_5 n(n+q)\epsilon_n^2 \\ & \lesssim n(n+q)\epsilon_n^2, \end{aligned}$$

Now, Lemma 9 of Jeong and Ghosal (2020) implies that for every $\epsilon > \epsilon_n$, there exists a test Φ_n such that

$$\begin{aligned} \mathbb{E}_0(\Phi_n) & \leq \frac{1}{2} \exp(b_6 n(n+q)\epsilon_n^2 - n(n+q)\epsilon^2/4), \\ \sup_{(\boldsymbol{\alpha}, \boldsymbol{\gamma}, \mathbf{Z}, \mathbf{B}) \in \mathcal{F}_n: H_n(\boldsymbol{\Theta}, \boldsymbol{\Theta}_0) > \epsilon} \mathbb{E}_\Theta(1 - \Phi_n) & \leq \exp(-n(n+q)\epsilon^2/4), \end{aligned}$$

for some constant $b_6 > 0$. To complete the proof, we choose $\epsilon = 4C_2\epsilon_n^2$ for $C_2 > \max(C'_1, b_6)$. \square

B.4 Corollary on Frobenius Norm Convergence

The general guarantee of distributional convergence can be translated into more interpretable metrics for specific models. For instance, for binary node attributes (the MIRT model), we can show that the estimated probabilities converge to the true probabilities in terms of the Frobenius norm.

Corollary S1 (Consistency for Bernoulli Node Variables). *Under the conditions of Theorem 2, for a Bernoulli node variable model, the posterior distribution for the matrix of dyadic probabilities converges in Frobenius norm:*

$$\lim_{n \rightarrow \infty} \mathbb{E}_0 \left[\Pr \left(\frac{1}{\sqrt{n(n+q)}} \|g^{-1}(\Theta) - g^{-1}(\Theta_0)\|_F > C_3 \epsilon_n \mid \mathbf{A}, \mathbf{Y} \right) \right] = 0,$$

for some constant $C_3 > 0$, where g^{-1} is the inverse logit function.

This corollary confirms that the proposed model consistently recovers the underlying probabilities of interactions and responses at the same near-optimal, adaptive rate, ensuring robust predictive performance.

To obtain the conclusion of corollary S1, we only need to proof the following lemma.

Lemma S5. (Lemma S10 of Loyal and Chen (2025)) *Let Θ_1 and Θ_2 be the log-odds matrices that define the probability measures of two Bernoulli joint latent space model such that $\mathbf{P}_1 = g^{-1}(\Theta_1)$ and $\mathbf{P}_2 = g^{-1}(\Theta_2)$ where $g^{-1}(\cdot)$ is the inverse logit function and is applied component-wise, then $\frac{1}{\sqrt{n(n+q)}} \|\mathbf{P}_1 - \mathbf{P}_2\|_F \lesssim H_n(\Theta_1, \Theta_2)$.*

proof of lemma S5. This result does not depend on the joint latent space model structure, only that the entries of the adjacency matrix and node variables are independent Bernoulli random variables. Let $p_{1ij} = [\mathbf{P}_1]_{ij}$ and $p_{2ij} = [\mathbf{P}_2]_{ij}$. The Hellinger distance between two Bernoulli random variables satisfies

$$\begin{aligned} h^2(\Theta_{1ij}, \Theta_{2ij}) &= \frac{1}{2} \left[(\sqrt{p_{1ij}} - \sqrt{p_{2ij}})^2 + (\sqrt{1-p_{1ij}} - \sqrt{1-p_{2ij}})^2 \right] \\ &= \frac{1}{2} \left[\left(\frac{1}{2} 2 |\sqrt{p_{1ij}} - \sqrt{p_{2ij}}| \right)^2 + \left(\frac{1}{2} 2 |\sqrt{1-p_{1ij}} - \sqrt{1-p_{2ij}}| \right)^2 \right] \\ &\geq \frac{1}{4} (p_{1ij} - p_{2ij})^2, \end{aligned}$$

where we used the fact that $|\sqrt{p_{1ij}} + \sqrt{p_{2ij}}| < 2$ and $|\sqrt{1-p_{1ij}} + \sqrt{1-p_{2ij}}|$ since $p_{1ij}, p_{2ij} \in [0, 1]$. As such

$$H_n^2(\Theta_1, \Theta_2) = \frac{2}{n+2q+1} \left(\sum_{i < i'} h^2(p_{1ii'}^A, p_{2ii'}^A) + \sum_{ij} h^2(p_{1ij}^Y, p_{2ij}^Y) \right) \gtrsim \frac{1}{n(n+q)} \|\mathbf{P}_1 - \mathbf{P}_2\|_F^2.$$

\square

References

Boucheron, S., Lugosi, G., and Massart, P. (2013). *Concentration Inequalities: A Nonasymptotic Theory of Independence*. Oxford University Press.

Ghosal, S., Ghosh, J. K., and van der Vaart, A. W. (2000). Convergence rates of posterior distributions. *The Annals of Statistics*, 28(2):500 – 531.

Ghosal, S. and van der Vaart, A. (2007). Convergence rates of posterior distributions for noniid observations. *The Annals of Statistics*, 35(1):192 – 223.

Jeong, S. and Ghosal, S. (2020). Posterior contraction in sparse generalized linear models. *Biometrika*, 108(2):367–379.

Loyal, J. D. and Chen, Y. (2025). A spike-and-slab prior for dimension selection in generalized linear network eigenmodels. *Biometrika*, page asaf014.

Ning, B., Jeong, S., and Ghosal, S. (2020). Bayesian linear regression for multivariate responses under group sparsity. *Bernoulli*, 26(3):2353 – 2382.

Schwartz, L. (1965). On bayes procedures. *Zeitschrift für Wahrscheinlichkeitstheorie und verwandte Gebiete*, 4(1):10–26.